# Constitutive Modeling of Discontinuous Carbon Fiber Polymer Composites

Hang-Ki Lee, Pakal Rahul-Kumar,
J. Michael Starbuck[*], George C. Jacob[**]
John D. Allen and Srdan Simunovic

Computational Materials Science Group
[*]Composite Materials Technology
Oak Ridge National Laboratory
[**] University of Tennessee

www-cms.ornl.gov

ornl
*Bringing Science to Life*

# Overview

- Material modeling
  - Micro-mechanics-based damage model
  - Fracture mechanics-based damage model
  - Delamination Model
  - Preform Modeling
- Progressive Crush Experiments
- Future Work

# http://www-cms.ornl.gov/composites/

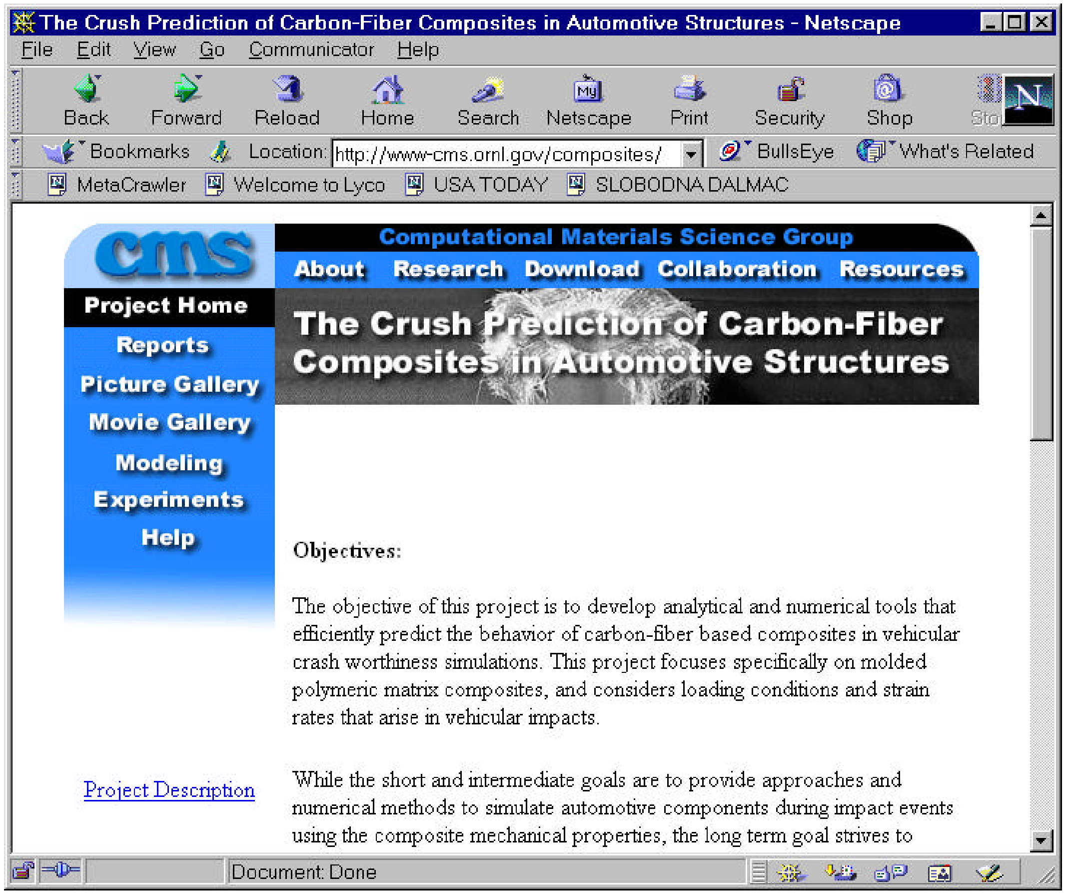


- Select ‘Reports’ for documentation



ornl
*Bringing Science to Life*

# Micromechanics-Based Constitutive Model of Discontinuous Fiber Composite Materials

**Haeng-Ki Lee and Srdan Simunovic**

Computational Materials Science Group
Oak Ridge National Laboratory
March 21, 2000

www-cms.ornl.gov

*Bringing Science to Life*

# Modeling of Discontinuous Fiber Composites

## Objective

Develop analytical and numerical tools for predicting mechanical response of discontinuous carbon fiber composites subjected to impact loading.

## Accomplishments

- Developed constitutive models based on micro-mechanical formulation and combination of micro- and macro-mechanical damage criteria.
- Incorporated developed models with probabilistic micro-mechanics for evolutionary damage in composite materials.
- Investigated effect of weakened interface (partial debonding) by employing an equivalent, transversely isotropic inclusion.
- Extended developed model to include crack effects on mechanical response of composite materials.

# Modeling of Discontinuous Fiber Composites

## † Accomplishments (Continued)

- Developed micromechanics-based inter-fiber interaction formulation for modeling of composites with high fiber volume fraction.
- Implemented models into finite element code DYNA3D to perform impact simulation of composite materials.
- Performed numerical simulations for Biaxial Test of Cruciform Shaped Composite Specimen and Four-point Bend Test in order to evaluate ability of developed composite model to predict experimentally obtained response.
- Performed parametric studies to evaluate constitutive model sensitivity to Weibull parameter $S_o$.

# Publications

1. Lee, H.K. and Simunovic, S., 2000. "Modeling of Progressive Damage in Aligned and Randomly Oriented Discontinuous Fiber Polymer Matrix Composites," *Composites Part B: Engineering*, Vol. 31 (no.2), 77-86.

2. Lee, H.K. and Simunovic, S., 2000. "A Damage Constitutive Model of Progressive Debonding in Aligned Discontinuous Fiber Composites," *International Journal of Solids and Structures,* accepted for publication.

3. Lee, H.K. and Simunovic, S., 1999. "A New Analytical Model for Impact Simulation of Random Fiber-reinforced Composites," submitted for journal publication to *Computer Methods in Applied Mechanics and Engineering*, assigned reference number CMAME #1271, in review.

4. Lee, H.K. and Simunovic, S., 1999, "A Micromechanical Constitutive Damage Model of Progressive Crushing in Random Carbon Fiber Polymer Composites," *ORNL/TM-1999/158,* 54 pages.

5. Lee, H.K. and Simunovic, S., 2000, "Constitutive Modeling and Impact Simulation of Random Carbon Fiber Polymer Matrix Composites for Automotive Applications," *2000 Future Car Congress,* April 2-6, Arlington, VA, paper number FCC-120, 6 pages, accepted.

# Publications


6. Lee, H.K. and Simunovic, S., 1999, “Constitutive Modeling for Impact Simulation of Random Fiber Composites,” *International Mechanical Engineering Congress & Expositions, The Winter Meeting of ASME*, AMD-Vol.17/NDE-Vol.17, pages 55-56.
7. Lee, H.K. and Simunovic, S., 1999, “Damage Behavior of Aligned and Random Fiber Reinforced Composites for Automotive Applications,” *SAMPE-ACCE-DOE Advanced Composites Conference*, September 27-28, Detroit, MI, pages 196-205.
8. Ju, J.W., Lee, H.K., and Simunovic, S., 1999, “Micromechanical Damage and Constitutive Modeling for Impact Simulation of Random Fiber Composite Structures,” *5th U.S. national Congress on Computational Mechanics*, August 4-6, Boulder, CO, page 119.
9. Lee, H.K. and Simunovic, S., 1999, “A Micromechanical Constitutive Model of Evolutionary Damage in Random Fiber Composites,” *6th International Conference on Composites Engineering*, June 27-July 3, Orlando, FL, pages 451-452.


* Papers are available at *http://www-cms.ornl.gov/composites/reports.html.*

# Outline

- Micromechanics-based Constitutive material model
- Progressive damage model
- Crack and inter-fiber interaction effects
- Finite element implementation for impact simulation
- Iterative algorithm for progressive damage model
- Biaxial impact simulation of cruciform shaped composite specimen
- Four-point bend simulation
- Summary and future directions

# Micromechanics and Equivalence Principle

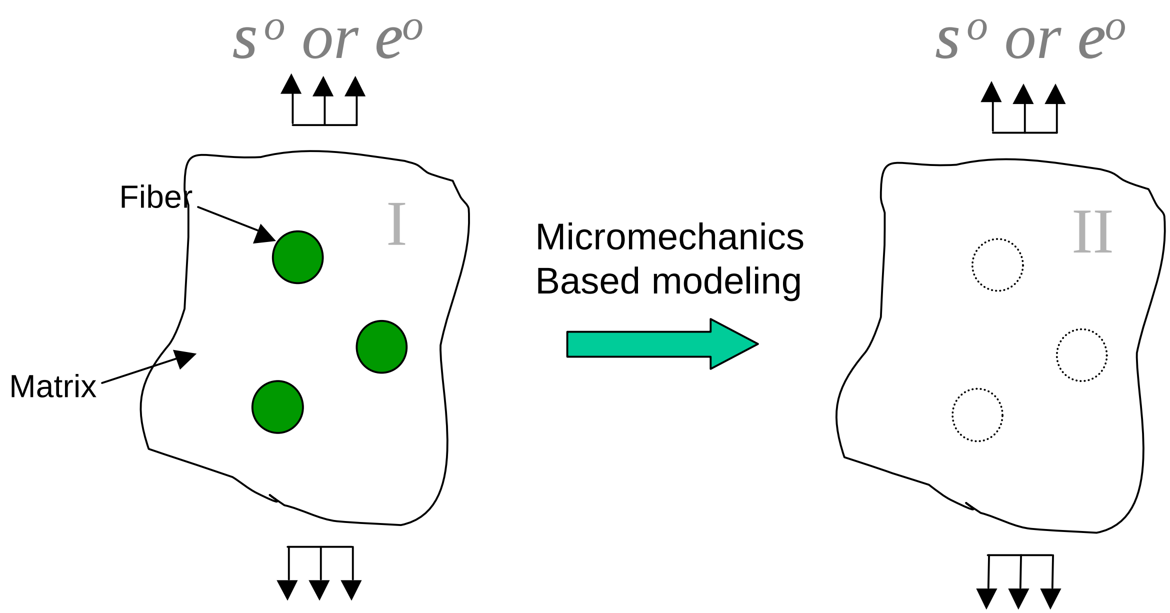


Heterogeneous composites

Equivalent homogeneous media with appropriately defined properties

# Composites with Aligned Discontinuous Fibers

- Effective elastic moduli of multi-phase composites containing randomly located, aligned elastic ellipsoids (*see publication #2*)

$$\mathbf{C}_* = \mathbf{C}_0 \cdot \left\{ \mathbf{I} + \mathbf{B} \cdot (\mathbf{I} - \mathbf{S} \cdot \mathbf{B})^{-1} \right\}$$

- Total stress at any point **x** in the matrix

$$\boldsymbol{\sigma}(\mathbf{x}) = \boldsymbol{\sigma}^o + \boldsymbol{\sigma}'(\mathbf{x})$$

in which $\boldsymbol{\sigma}^o$ and $\boldsymbol{\sigma}'$ are defined as

$$\boldsymbol{\sigma}^o \equiv \mathbf{C}_0 : \epsilon^o$$

$$\boldsymbol{\sigma}'(\mathbf{x}) \equiv \mathbf{C}_0 : \int_V \mathbf{G}(\mathbf{x} - \mathbf{x}') : \epsilon_1^*(\mathbf{x}')\, d\mathbf{x}' + \mathbf{C}_0 : \int_V \mathbf{G}(\mathbf{x} - \mathbf{x}') : \epsilon_2^*(\mathbf{x}')\, d\mathbf{x}'$$

# Composites with Aligned Discontinuous Fibers

- Ensemble-averaged stress norm for any matrix point **x**

$$\langle H \rangle_m(\mathbf{x}) \cong H^o + \int_{|\mathbf{x}-\mathbf{x}_1^{(1)}|>a} \left\{ H(\mathbf{x}|\mathbf{x}_1^{(1)}) - H^o \right\} P(\mathbf{x}_1^{(1)})\, d\mathbf{x}_1^{(1)} + \int_{|\mathbf{x}-\mathbf{x}_2^{(1)}|>a} \left\{ H(\mathbf{x}|\mathbf{x}_2^{(1)}) - H^o \right\} P(\mathbf{x}_2^{(1)})\, d\mathbf{x}_2^{(1)} + \ldots..$$

- Effective yield function for fiber-reinforced composites

$$\bar{F} = (1-\phi_1)^2 \bar{\boldsymbol{\sigma}} : \bar{\mathbf{T}} : \bar{\boldsymbol{\sigma}} - K^2(\bar{e}^p)$$

where the isotropic hardening function $K(\bar{e}^p)$ is defined as

$$K(\bar{e}^p) = \sqrt{\frac{2}{3}} \left\{ \sigma_y + h(\bar{e}^p)^{\bar{q}} \right\}$$

# Randomly Oriented, Discontinuous Fibers

- Orientational averaging process (*see publication #1*)

$$\subset \cdot \supset \equiv \int_0^{2\pi} \int_0^{\pi/2} (\cdot) P(\theta, \phi) sin\theta d\theta d\phi$$

- Governing equations for randomly oriented fiber-reinforced composites

$$\subset \bar{\boldsymbol{\sigma}} \supset = \mathbf{C}_0 : [\subset \bar{\boldsymbol{\epsilon}} \supset - \sum_{r=1}^{2} \phi_r \subset \boldsymbol{\epsilon}_r^* \supset]$$

$$\subset \bar{\boldsymbol{\epsilon}} \supset = \boldsymbol{\Upsilon} : \boldsymbol{\epsilon}^o$$

$$\subset \boldsymbol{\epsilon}_r^* \supset = -\boldsymbol{\Omega}_r : \boldsymbol{\epsilon}^o$$

# Progressive Damage Model

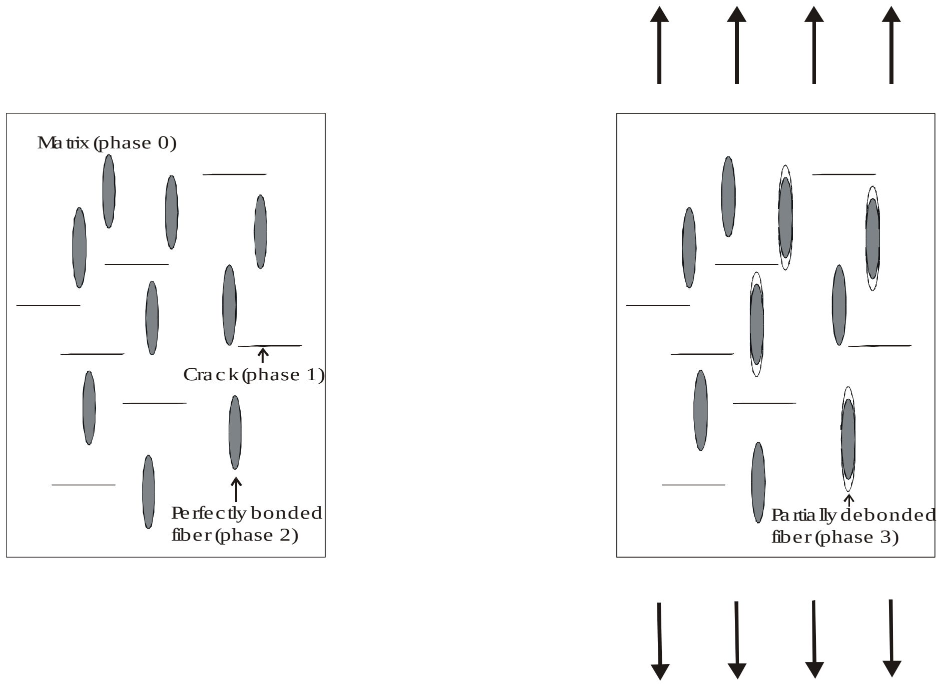


The initial state

The damaged state

✝ A schematic of aligned fiber composites subjected to uniaxial tension.

# Equivalence Principle for Partially Debonded Fibers

See Figure A.

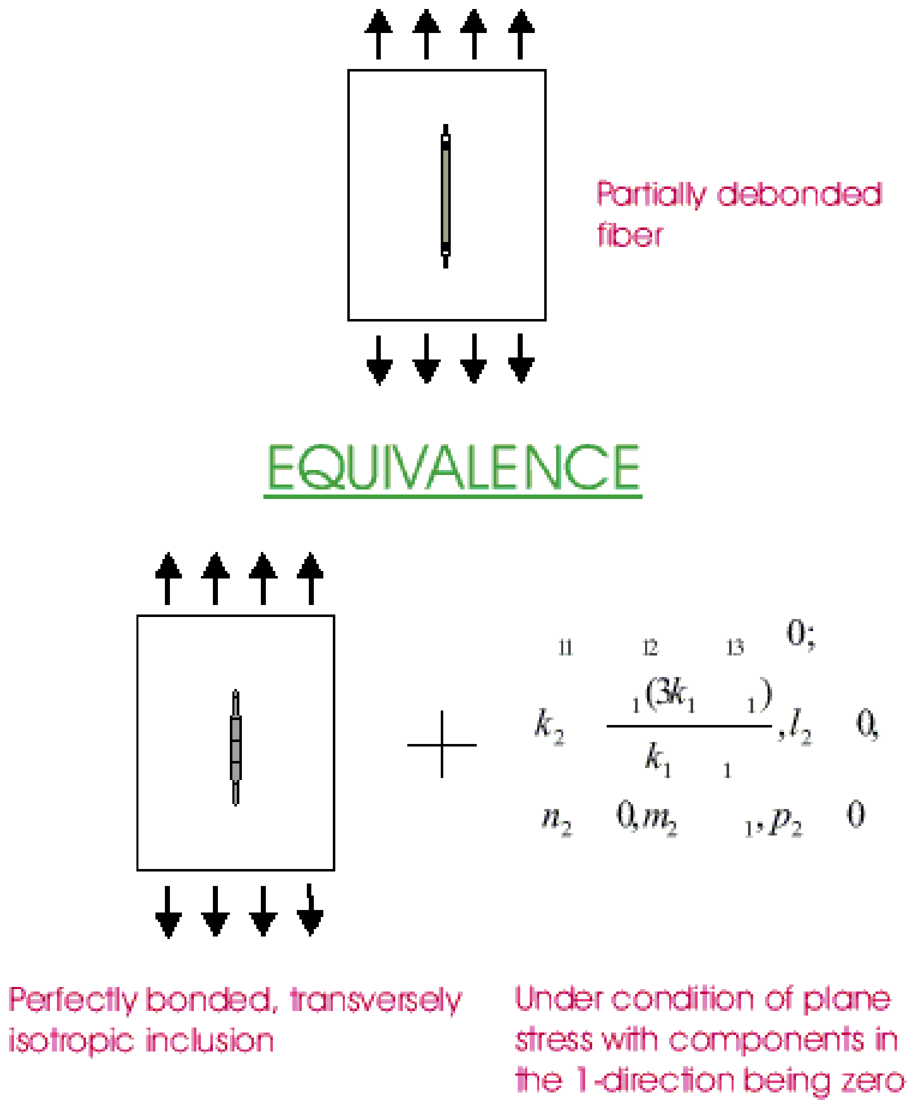


Figure A. A schematic of the equivalence between a partially debonded fiber and an equivalent perfectly bonded, transversely isotropic inclusion.

# Progressive Damage Model

- Weibull probabilistic distribution function for fiber debonding (damage)

$$P_d[(\bar{\boldsymbol{\sigma}}_m)_1] = 1 - exp\left[-\left(\frac{(\bar{\boldsymbol{\sigma}}_m)_1}{S_o}\right)^M\right]$$

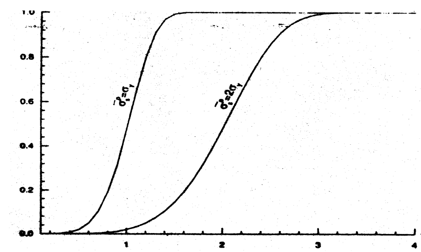


- Current debonded (damaged) fiber volume fraction

$$\phi_2 = \phi P_d[(\bar{\boldsymbol{\sigma}}_m)_1] = \phi\left\{1 - exp\left[-\left(\frac{(\bar{\boldsymbol{\sigma}}_m)_1}{S_o}\right)^M\right]\right\}$$

# Penny-Shaped Cracks

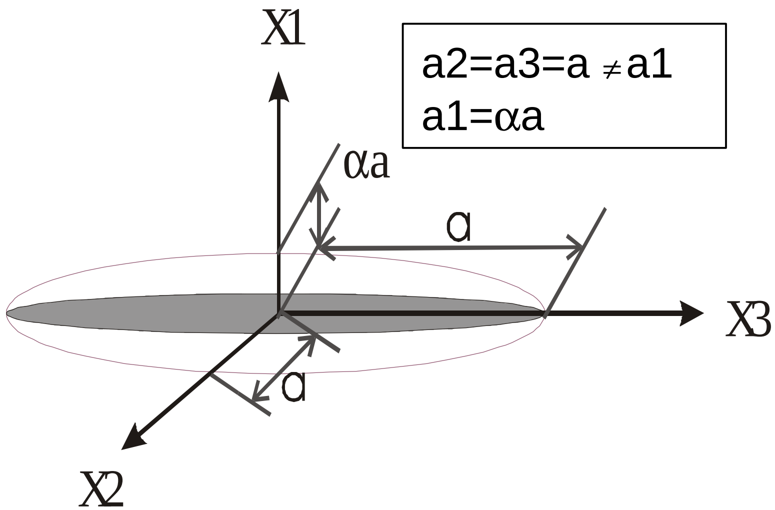


Spheroidal inclusion

If $a$>1; prolate spheroidal inclusion
$a$=1; spherical inclusion
$a$<1; oblate spheroidal inclusion

- Penny-shaped cracks are regarded as the limiting case of oblate spheroidal voids with aspect ratio $a \longrightarrow 0$.
- Various cracks with different crack size and orientation can be included into the constitutive model by adding the corresponding inclusion phases.
- Penny-shaped cracks are assumed to remain at the same crack density during the deformations.
- Effective elastic moduli for multi-phase composites containing various cracks is derived as (*see publication #3*):

$$C_* = C_o \cdot \left[ I + \sum_{r=1}^{n} \{ f_r (A_r + S_r)^{-1} \cdot [I - f_r S_r \cdot (A_r + S_r)^{-1}]^{-1} \} \right]$$

# Effect of Cracks on Mechanical Behavior of Composite

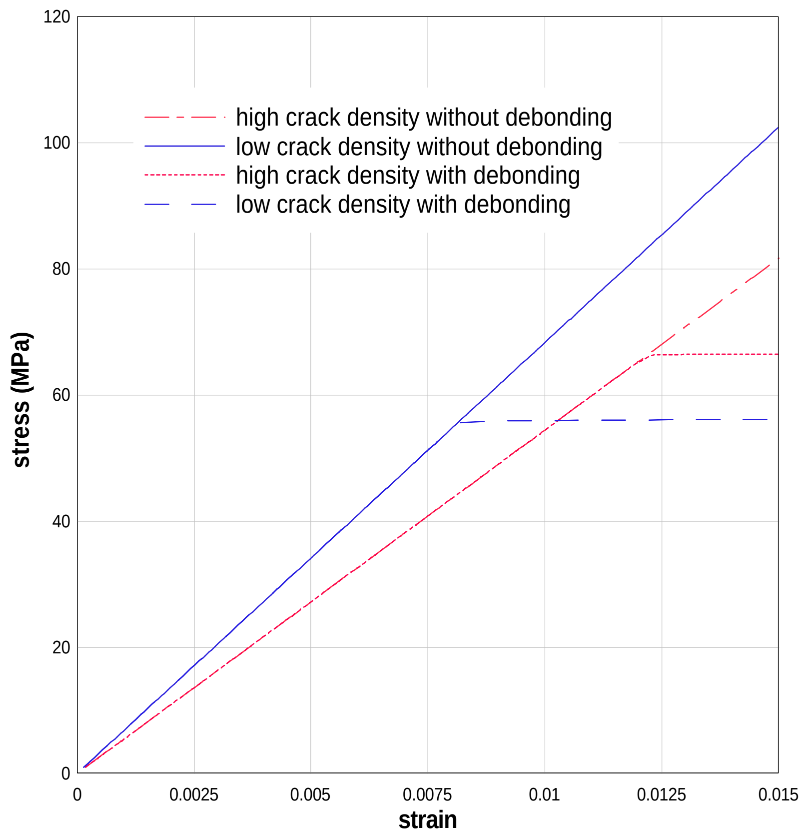

# Inter-Fiber Interaction Formulation

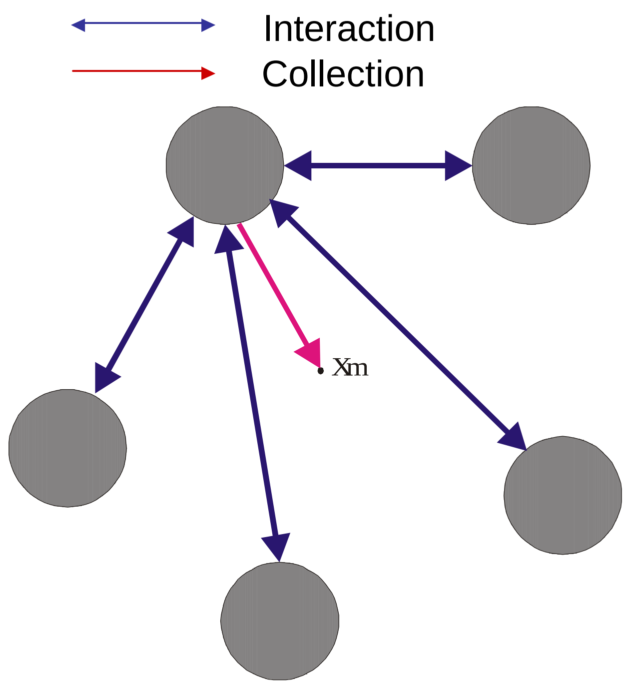


Local matrix point $x_m$ collects stress perturbations due to surrounding fibers with pairwise inter-fiber interaction.

- Approximate eigenstrain accounting for pairwise fiber interaction for multi-phase composites

$$< e^{*} >= \Gamma : e^{*o}$$

- Effective elastic moduli for multi-phase composites considering inter-fiber interaction (*The corresponding paper is in preparation.*)

$$C_{*} = C_{o} \cdot \{ I - \sum_{r=1}^{n} [ f_r \Gamma \cdot ( A_r - S_r + f_r S_r \cdot \Gamma )^{-1} ] \}$$

# Inter-Fiber Interaction Formulation

Title:
cont1.eps
Creator:
haengki@capsicum with xmgr
Preview:
This EPS picture was not saved
with a preview included in it.
Comment:
This EPS picture will print to a
PostScript printer, but not to
other types of printers.

Title:
cont2.eps
Creator:
haengki@capsicum with xmgr
Preview:
This EPS picture was not saved
with a preview included in it.
Comment:
This EPS picture will print to a
PostScript printer, but not to
other types of printers.

- Inter-fiber interactions significantly affect the overall composite moduli when the contrast ratio is high (or low).

# Finite Element Implementation for Impact Simulation

- Model is implemented into finite element code DYNA3D to perform impact simulation of composite materials.
- Model uses strain driven algorithm to link with displacement based finite element code DYNA3D.
- Micromechanical iterative algorithm is used for modeling progressive damage.

# Iterative Algorithm for Progressive Damage Model

See Box 1.

**Box 1** Iterative algorithm for progressive damage model

(i) Compute (see Probabilistic approach for progressive damage) :

Damaged (Partially debonded) fiber material properties : $k_3, l_3, m_3, n_3, p_3$

(ii) Estimate model parameters (refer to Parameter estimation algorithm) :

Plastic material parameters : $\sigma_y,\ h,\ \bar{q}$;   Weibull parameters : $S_o,\ M$

(iii) Initialize : set $z = 0$; $(\phi_1)^{(0)}_{n+1} = (\phi_1)_n,\ (\phi_2)^{(0)}_{n+1} = (\phi_2)_n$

(iv) Compute (see Constitutive material model formulations) :

Effective moduli : $(\kappa_*)^{(z)}_{n+1},\ (\mu_*)^{(z)}_{n+1},\ (E_*)^{(z)}_{n+1},\ (\nu_*)^{(z)}_{n+1}$;

Internal stresses of fibers : $[(\bar{\sigma}_m)_1]^{(z)}_{n+1}$

(v) Compute the Weibull probability distribution function :

$$P_d\left\{[(\bar{\sigma}_m)_1]^{(z)}_{n+1}\right\} = 1 - exp\left[-\left(\frac{[(\bar{\sigma}_m)_1]^{(z)}_{n+1}}{S_o}\right)^M\right]$$

(vi) Compute volume fractions :

$$(\phi_2)^{(z)}_{n+1} = \phi P_d\{[(\bar{\sigma}_m)_1]^{(z)}_{n+1}\} = \phi\left\{1 - exp\left[-\left(\frac{[(\bar{\sigma}_m)_1]^{(z)}_{n+1}}{S_o}\right)^M\right]\right\},$$

$$(\phi_1)^{(z)}_{n+1} = \phi - (\phi_2)^{(z)}_{n+1}$$

(vii) Perform convergence check :

If $\left|\dfrac{(\phi_1)^{(z)}_{n+1} - (\phi_1)^{(z-1)}_{n+1}}{(\phi_1)^{(z-1)}_{n+1}}\right| \leq TOL\ \ (e.g.,\ 10^{-8})$ : then update quantities in (iv), (vi)

$[(\bar{\sigma}_{ii})_1]_{n+1} = [(\bar{\sigma}_{ii})_1]^{(z)}_{n+1},\ (i = 1, 2, 3);$

$(\phi_1)_{n+1} = (\phi_1)^{(z)}_{n+1},\ (\phi_2)_{n+1} = (\phi_2)^{(z)}_{n+1}$;   GO TO (viii) in **Box 2**.

Otherwise : SET $z = z + 1$; GO TO (iv).

# Return Mapping Algorithm

See Box 2.

**Box 2**. 3-D return mapping algorithm

(viii) 3D return mapping algorithm (based on strain driven algorithm) :

(a) Initialize : set $l = 0$; $(\bar{\boldsymbol{\epsilon}}^p_{n+1})^{(0)} = \bar{\boldsymbol{\epsilon}}^p_n$, $(\bar{e}^p_{n+1})^{(0)} = \bar{e}^p_n$ (for local Newton iteration)

(b) Compute : $\bar{\boldsymbol{\sigma}}_n = \mathbf{C}_n : [\bar{\boldsymbol{\epsilon}}_n - \bar{\boldsymbol{\epsilon}}^p_n]$

(c) Compute the elastic predictor :

Trial elastic state : $\bar{\boldsymbol{\sigma}}^{tr}_{n+1} = \bar{\boldsymbol{\sigma}}_n + \mathbf{C}_n : \Delta\boldsymbol{\epsilon}_{n+1}$

Compute : $\bar{\boldsymbol{\epsilon}}_{n+1} = \bar{\boldsymbol{\epsilon}}_n + \Delta\boldsymbol{\epsilon}_{n+1}$;

$$\bar{F}^{tr}_{n+1}(\bar{\boldsymbol{\sigma}}^{tr}_{n+1}, \bar{e}^p_n) = (1 - (\phi_1)_{n+1})^2 \bar{\boldsymbol{\sigma}}^{tr}_{n+1} : \bar{\mathbf{T}}_{n+1} : \bar{\boldsymbol{\sigma}}^{tr}_{n+1} - K^2(\bar{e}^p_n)$$

(d) Check whether plastic loading is active :

If $\bar{F}^{tr}_{n+1} \leq TOL$ (elastic step; e.g., $TOL = 10^{-8}$) :

$\hat{\xi}_{n+1} = 0$; SET $\bar{\boldsymbol{\sigma}}_{n+1} = \bar{\boldsymbol{\sigma}}^{tr}_{n+1}$, $\bar{e}^p_{n+1} = \bar{e}^p_n$; GO TO (iv) in **Box 1**.

Otherwise (plastic step) : GO TO (e).

(e) Perform plastic correction; return mapping algorithm :

Solve nonlinear scalar equation for $\hat{\xi}_{n+1}$: use local Newton iteration

$$\bar{F}_{n+1}(\hat{\xi}^{(l)}_{n+1}) = [1 - (\phi_1)_{n+1}]^2 \bar{\boldsymbol{\sigma}}^{(l)}_{n+1} : \bar{\mathbf{T}}_{n+1} : \bar{\boldsymbol{\sigma}}^{(l)}_{n+1} - K^2[(\bar{e}^p_{n+1})^{(l)}] = 0$$

(f) Perform convergence check :

If $|\bar{F}_{n+1}[(\hat{\xi}_{n+1})^{(l)}]| \leq TOL$ ($e.g.,\ 10^{-8}$) : then update

$$\hat{\xi}_{n+1} = \hat{\xi}^{(l)}_{n+1},\ \bar{\boldsymbol{\sigma}}_{n+1} = \bar{\boldsymbol{\sigma}}^{(l)}_{n+1},\ \bar{\boldsymbol{\epsilon}}^p_{n+1} = (\bar{\boldsymbol{\epsilon}}^p_{n+1})^{(l)},\ \bar{e}^p_{n+1} = (\bar{e}^p_{n+1})^{(l)};\ \text{EXIT}.$$

Otherwise : SET $l = l + 1$

Compute derivative of $\bar{F}[(\hat{\xi}_{n+1})^{(l)}]$ : $D\bar{F}[(\hat{\xi}_{n+1})^{(l)}]$

$$(\hat{\xi}_{n+1})^{(l+1)} = (\hat{\xi}_{n+1})^{(l)} - \frac{\bar{F}[(\hat{\xi}_{n+1})^{(l)}]}{D\bar{F}[(\hat{\xi}_{n+1})^{(l)}]};\quad \text{GO TO (e)}.$$

# Cantilever Composite Beam under Impact

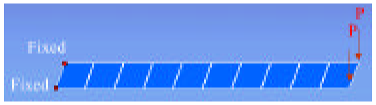


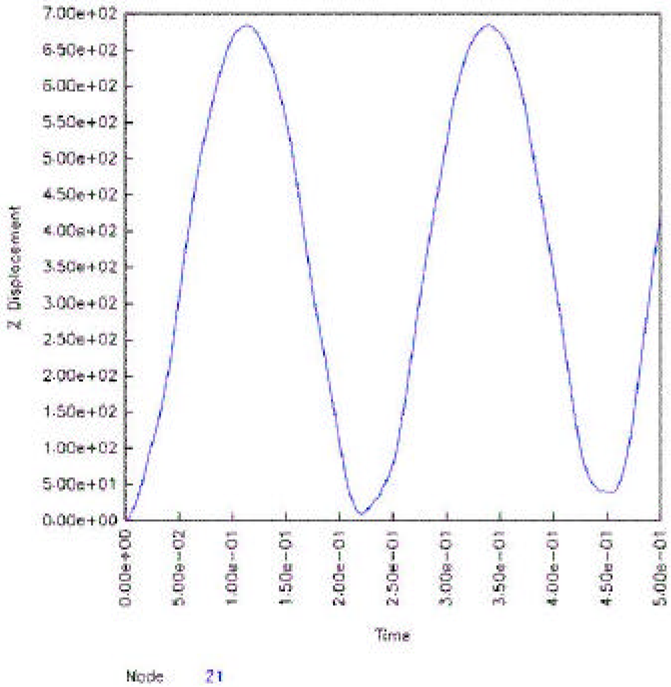


Displacement at the free edge during impact

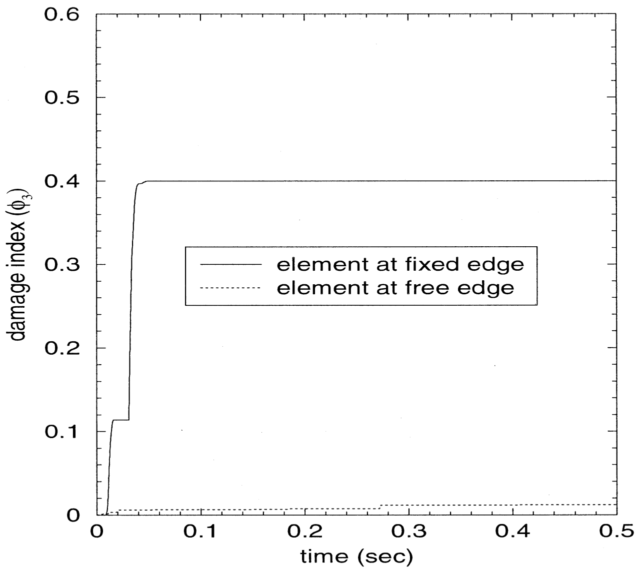


Damage index, representing the volume fraction of damaged fibers, at free and fixed edges during impact

# Biaxial Test Simulations

- Planar biaxial tests of cruciform shaped composite specimen were performed by Waas and Quek (1999) to gain insight into constitutive behavior of damage induced composite materials.
- Numerical simulations of biaxial tests were carried out to examine whether the implemented computational model is able to predict the experimentally obtained response.
- Composite specimen was loaded proportionally with the rate of 30 lb/sec (130 N/sec) in biaxial compression and tension in the ratio of 1:1.
- Material properties, volume fraction of fibers, and aspect ratio of fibers were $E_m$=3.0GPa, $n_m$=0.35, $E_f$=72GPa, $n_f$=0.17, $f$=0.5, and $a$ =20.0. Default DYNA3D shell element formulation based on Belyschko-Tsay theory was utilized for modeling the composite specimen.

# Biaxial Test Simulations

See Figures 1 and 2.

# Damage Contours During Biaxial Loading

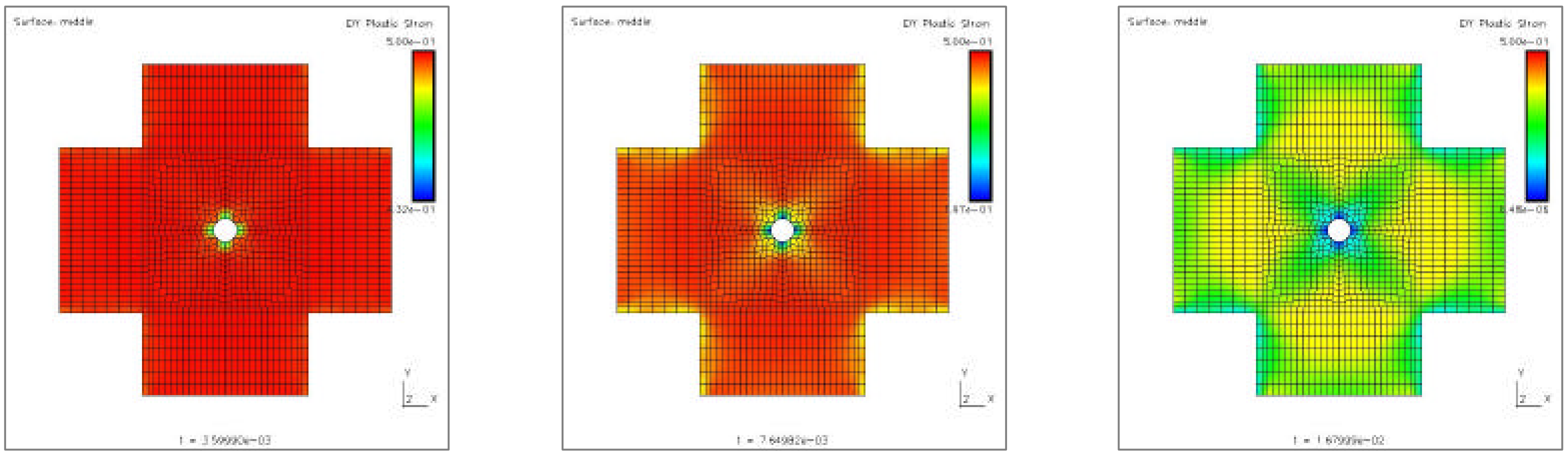


- Figures show a sequence of damage contours during biaxial loading. Damage zone emanates from the edges of the cutout.
- Figure 2 of previous slide and above figures show damage initiation and evolution along the *x*- and *y*-axes around the cutout, which corresponds to Waas and Quek [1] 's observations.
- Simulations are used for predicting the direction and the rate of damage propagation during the test.

# Four-Point Bend Simulation

- For progressive crush tests of composite tubes, flexural properties and the corresponding damage mechanisms of components must be characterized.
- Four-point bend test is commonly used for determining the flexural properties of high-strength composites.
- To assess the predictive capability of the computational model for simulating impact damage of composite structures, numerical four-point bend simulations were carried out.
- In order to avoid excessive indentation, or failure due to stress concentration directly under the loading nose, the loading nose in contact with the specimen must be sufficiently large.
- Rigid loading noses and rigid supports were modeled as the master surface and the set of nodes on the composite plate as the slave contact node set.

# Four-Point Bend Simulation

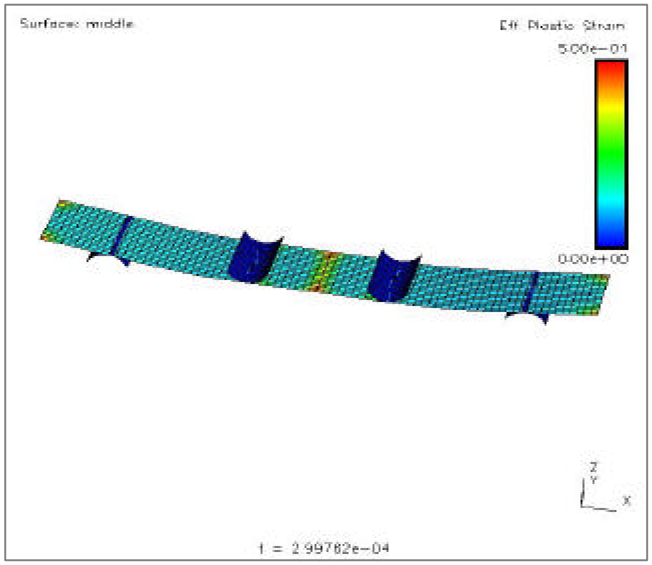


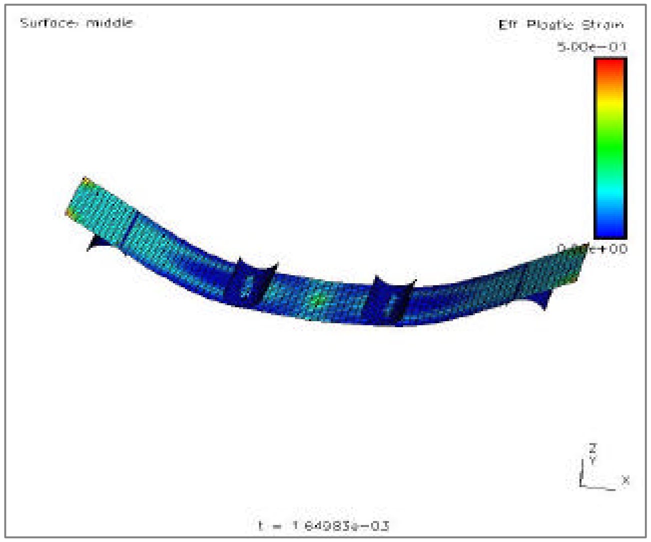


Sequence of damage contours and deformed shape during four-point bend impact

- Figures show the maximum damage at surfaces located around loading noses.



ornl
*Bringing Science to Life*

# Four-Point Bend Simulation

Title:
com2.eps
Creator:
haengki@capsicum with xmgr
Preview:
This EPS picture was not saved
with a preview included in it.
Comment:
This EPS picture will print to a
PostScript printer, but not to
other types of printers.

Time-history plots for the damage index at the contact surface near loading nose and at the center between loading nose and support

† Simulation will be performed with a geometrical trigger at the center of the specimen.

# Parametric Study for Weibull Parameter $S_o$

Title:
d327.eps
Creator:
haengki@capsicum with xmgr
Preview:
This EPS picture was not saved
with a preview included in it.
Comment:
This EPS picture will print to a
PostScript printer, but not to
other types of printers.

$\sigma_y$: yield stress of the matrix

Damage index, representing the volume fraction of perfectly bonded fibers, during four-point loading

† Influence of the value of Weibull parameter $S_o$, which is related to the interfacial strength, on the damage evolution in composite.

# Summary

- Emanating from a constitutive damage model for aligned fiber-reinforced composites, a micromechanical damage constitutive model for random fiber-reinforced composites was developed to perform impact simulation of random fiber-reinforced composites for automotive applications.
- Evolutionary interfacial debonding model and a crack-weakened model were subsequently employed in accordance with the Weibull's probability function to characterize the varying probability of fiber debonding.
- Micromechanics-based inter-fiber interaction formulation has been developed to model composites with high fiber volume fraction.
- Developed constitutive model is able to simulate mechanical behavior of new composite materials (e.g., P4) containing cracks of different sizes and orientations by adding the corresponding inclusion phases.

# Summary

- Constitutive models were implemented into the nonlinear finite element code DYNA3D using a user-defined material subroutine to simulate the dynamic inelastic behavior and the progressive damage of the composite materials.
- Composite impact simulations were carried out to predict the experimentally obtained response during impact.
- Based on the numerical simulations, we can draw the conclusion that although more experimental work is needed to determine the damage parameters, the implementation of a new constitutive model into the finite element code DYNA3D has resulted in a promising numerical tool for the simulation of progressive damage in impacted composite structures.

# Future Directions

- Develop laboratory experiments and procedures for characterizing basic damage mechanisms and monitoring the damage evolution during impact using nondestructive evaluation techniques.
- Conduct further assessment and experimental validation of the developed damage models to simulate composite crushing problems.

# Fracture Mechanics Based Damage Modeling of RFC Composites

**Pakal Rahul-Kumar**
**Srdan Simunovic**
**Computational Material Science Group**
**Oak Ridge National Laboratory**

**21 March, 2000**

# Damage Modeling of RFC Composites

- Prone to failure by accumulation of damage and growth of cracks
- The failures have origins in microstructural defects such as
  - Micro-cracks in matrix material
  - Weak material interfaces
  - Voids and secondary crack surfaces
- Mechanical performance is directly related to resist failure by crack initiation and subsequent growth, i.e. the *Fracture Toughness* of the material

# Damage Modeling of RFC Composites

- Build upon existing theories that account for the microstructure of the material
- Allow for the evolution of the microstructure by employing the governing physical laws
- Model the stress relaxation/softening with evolving microstructure
- Use traditional fracture mechanics based testing methods to calibrate the model

# Properties of Micro-cracked Solids

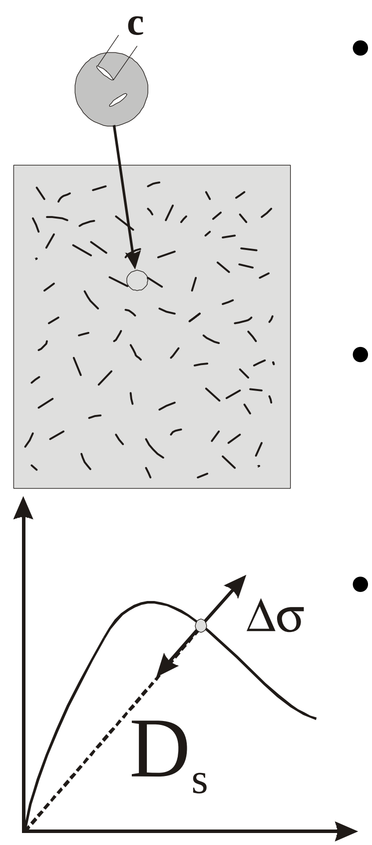


- Several studies in literature focused on the prediction of properties of micro-cracked solids
- Studies take into account the micro-crack opening, frictional sliding, crack interaction
- Consider only a *stationary system* of micro-cracks. Examples are the
  - Self Consistent scheme
  - Differential Scheme

# Existing Theories - Secant Moduli

- Differential Scheme Estimates (Hashin 1988)

$$\rho = \frac{5}{8}\ln\frac{\nu}{\nu_e} + \frac{15}{64}\ln\left(\frac{1-\nu_e}{1-\nu}\right) + \frac{45}{128}\ln\left(\frac{1+\nu_e}{1+\nu}\right) + \frac{5}{128}\ln\left(\frac{3-\nu_e}{3-\nu}\right)$$

$$E_e = E\left(\frac{\nu_e}{\nu}\right)^{10/9}\left(\frac{3-\nu}{3-\nu_e}\right)^{1/9}$$

Crack density, $\rho = Nc^3$

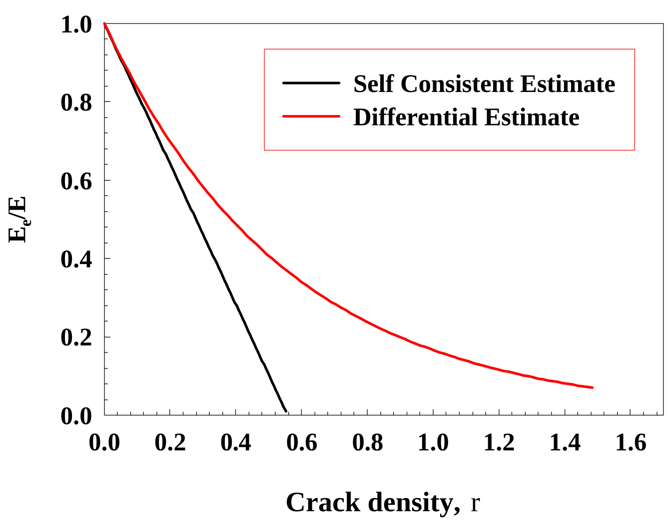


- Self Consistent Estimates (Budiansky & O'Connell, 1976)

$$E_e = E\left(1-\rho\frac{16(1-\nu^2)(10-3\nu)}{45(2-\nu)}\right)$$

$$\nu_e = \nu\left(1-\rho\frac{16(1-\nu^2)(3-\nu)}{15(2-\nu)}\right)$$



ornl
*Bringing Science to Life*

# Evolving Microstructure

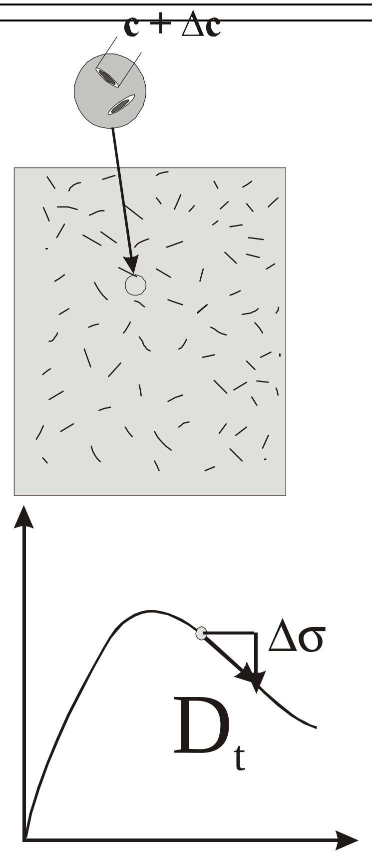


- During material failure, exiting micro-cracks grow in size, new micro-cracks are formed, and they subsequently interact and coalesce

- Energy absorbed is determined by these failure mechanisms which affect the post-failure response

- In computational modeling
  - Need to estimate the tangent moduli $D_t$ for an evolving system of micro-cracks
  - Capture stresses relaxation accompanying accumulation of damage

# Rate Constitutive Relations

- Constitutive relation for elastic material with micro-cracks distributed statistically uniformly

$$\sigma = D_s(c, N) : \varepsilon$$

- Rate equations for evolving microstructure are obtained as

$$\dot{\sigma} = D_s : \dot{\varepsilon} + \dot{D}_s : \varepsilon = D_e : \dot{\varepsilon} + \frac{\partial D_s}{\partial c}\dot{c} : \varepsilon + \frac{\partial D_s}{\partial N}\dot{N} : \varepsilon$$

- Constitutive description is complete by specifying
  - Micro-crack growth rate, $\dot{c}$
  - Micro-crack nucleation rate, $\dot{N}$

# Micro-Crack Growth & Nucleation Rates

Experimental observations reveal

– Cracks grow at a fraction of Raliegh surface wave speed (Ravi-Chandar & Knauss 1984, Freund 1998)

$$\dot{c} = \alpha(\sigma) v_R, \quad \alpha < 1.0 \quad v_s = \sqrt{\frac{E_e}{2\rho(1+\nu)}}, \quad v_R = v_s \frac{0.862 + 1.14\nu_e}{1+\nu_e}$$

– Crack nucleation is governed as (Seaman et al.,1976)

$$\dot{N} = \dot{N}_0 \exp\left(\frac{P - P_0}{P_1}\right), \quad P > P_0 \qquad \dot{N} = 0, \; P \le P_0$$



Bringing Science to Life

# Micro-Crack Stability

- Micro-crack stability is governed by energy balance as specified by Griffith fracture theory
- The stress state, normal and shear stresses, surrounding a crack tip governs the crack driving energy, G

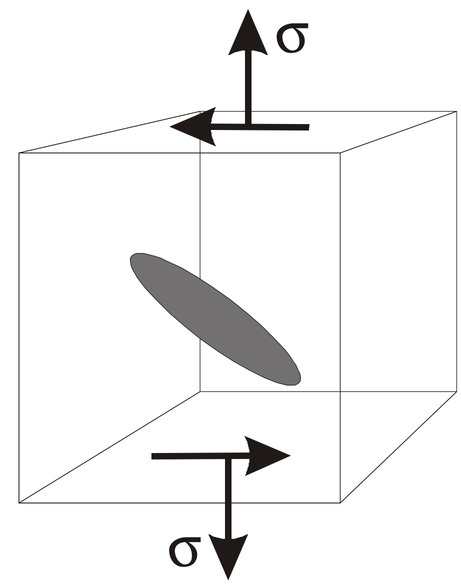


- Cracks growth when crack driving energy G is greater than the fracture toughness of material, $\Gamma_R$

# Stresses on a Micro-Crack

- Normal traction on a micro-crack

$$\sigma_n = \sigma_{ij} n_i n_j$$

- Shear traction on a micro-crack

$$\sigma_t = \left[ \sigma_{ij} n_j \sigma_{ik} n_k - \left( \sigma_{ij} n_i n_j \right)^2 \right]^{1/2}$$

- Frictional resistance stress are

$$\sigma_r = \sigma_0 - \mu \left( \sigma_{ij} n_i n_j \right)$$

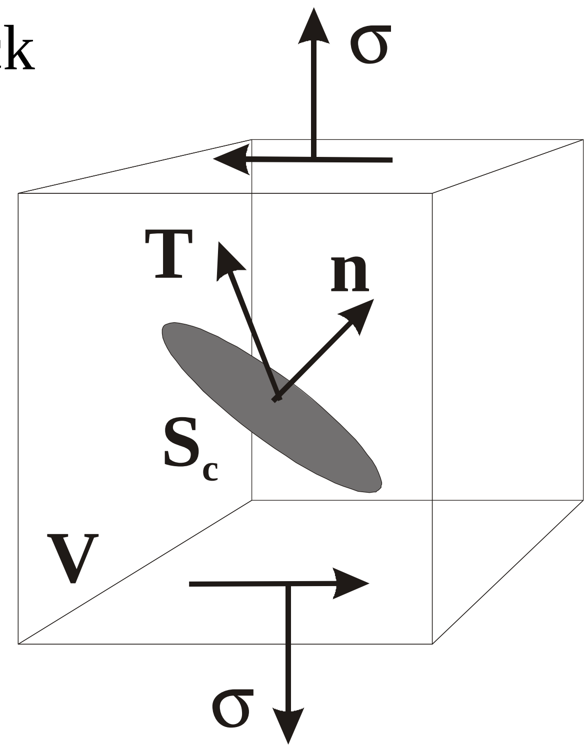




ornl
Bringing Science to Life

# Micro-Crack Stability Criteria

Application of Griffith Criteria for a penny shaped micro-crack results in the following crack stability criteria (Addessio & Johnson 1990)

- Crack growth under tension $\left(\sigma_n = \sigma_{ij} n_i n_j \geq 0\right)$

$$F_n\left(\sigma_{ij}, n_i, c\right) = \sigma_{ij} n_j \sigma_{ik} n_k - \frac{\nu}{2}\left(\sigma_{ij} n_i n_j\right)^2 - \overline{K}/c \geq 0$$

- Crack growth under compression $\left(\sigma_n = \sigma_{ij} n_i n_j < 0\right)$

$$F_t\left(\sigma_{ij}, n_i, c\right) = \left(\sigma_t - \sigma_r\right)^2 - \overline{K}/c \geq 0$$

$$\overline{K} = \frac{\pi}{2}\left(\frac{2-\nu}{1-\nu}\right)\frac{\Gamma_R G}{c}$$

# Damage Surfaces

- Continuum level representation of micro-crack stability criteria is a *damage surface* and is obtained through the following volume average procedure (Addessio & Johnson 1990)

$$\iiint_{Vc\Omega} F\left(\sigma_{ij}, n_i, c\right) w\left(c, \Omega\right)\, dc d\Omega dV \geq 0$$

w(c,Ω) – Crack distribution function

- The resulting damage surface are defined in terms of the scalar parameters, p and q, defined as

$$p = -\frac{1}{3}\sigma_{ii} \quad \text{and} \quad q = \left(\frac{3}{2}s_{ij}s_{ij}\right)^{1/2}, s_{ij} = \sigma_{ij} + p\delta_{ij}$$

# Damage Surfaces

(Addessio & Johnson 1990)

- In tension, $p < 0$, damage surface is obtained as

$$q^2 + \frac{45}{4(5-\nu)}\left[(2-\nu)p^2 - \frac{2\overline{K}}{c}\right] = 0$$

- In compression, $p > 0$, damage surface is obtained as

$$q^2 - \frac{45}{3(3-2\mu^2)}\left[\left(\mu p + \sigma_0 + \sqrt{\frac{\pi\overline{K}}{\overline{c}}}\right) + \frac{2\overline{K}}{\overline{c}}\right] = 0$$



ornl
*Bringing Science to Life*

# Damage Surfaces

Graphical plot of the damage surface in the (p,q,c) space

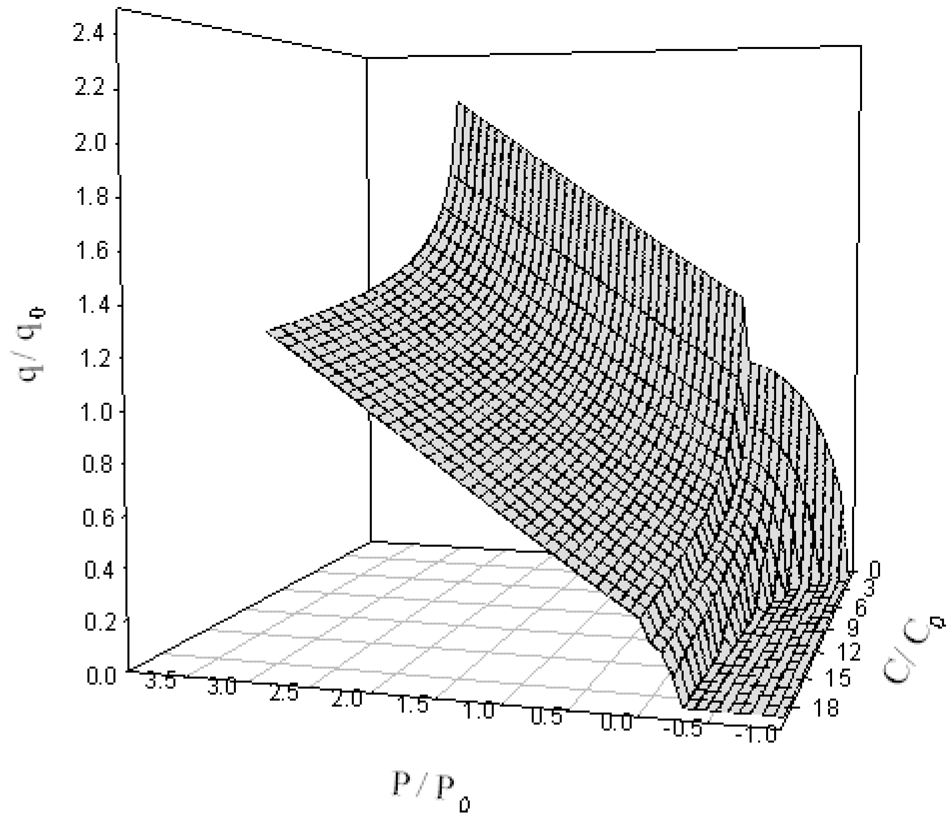




Bringing Science to Life

# Damage Surfaces

Graphical plots of the damage surface in the (p,q) space for various fixed values of micro-crack length, c

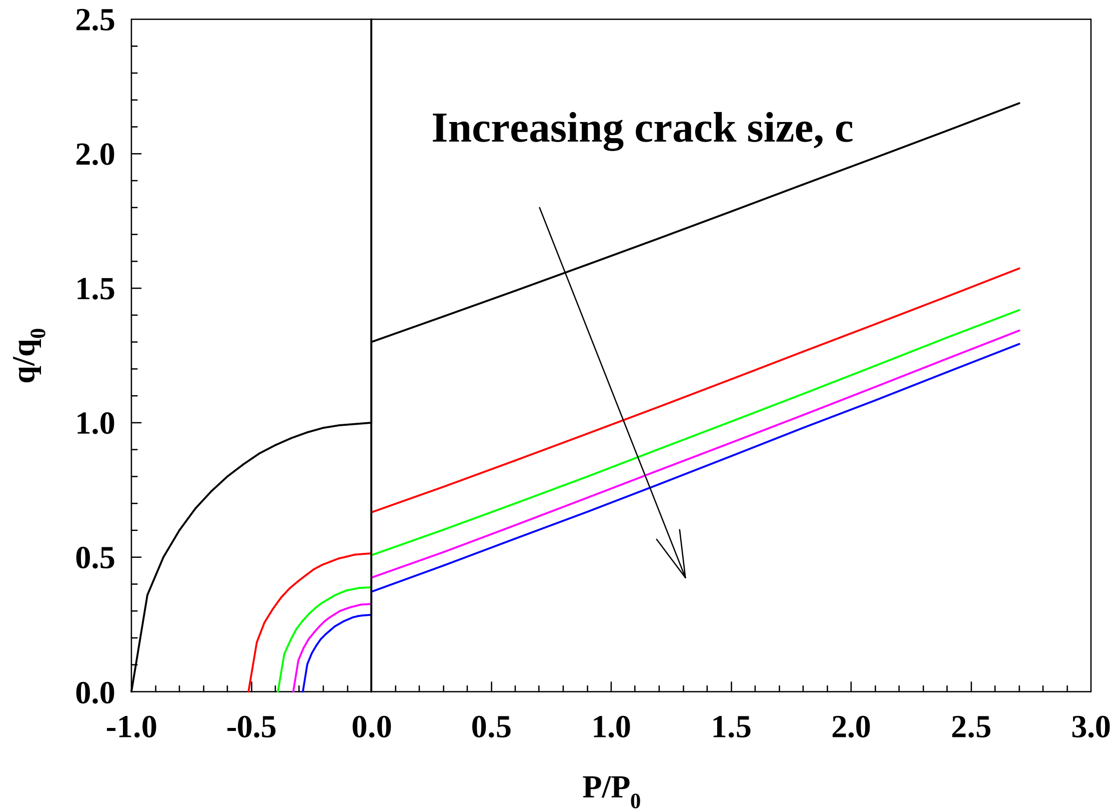


Bringing Science t

l.gov

# Dissipative Nature of Material

- As cracks grow crack distribution evolves and the stiffness/compliance varies in time

$$\dot{\varepsilon} = C_e : \dot{\sigma} + \dot{C}_e : \sigma$$

- Rate equation for a Maxwell solid

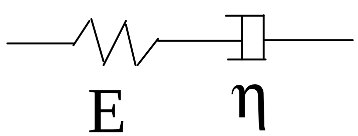


$$\dot{\varepsilon} = \frac{\dot{\sigma}}{E} + \frac{\sigma}{\eta}$$

- Material behaves as a Maxwell solid with a variable relaxation time, $\tau$

$$\tau = \frac{\eta}{E} = \frac{C_e}{\dot{C}_e}$$

# Material Point Constitutive Algorithm

1. Initialize: $c_{n+1} = c_n$, $\varepsilon_{n+1} = \varepsilon_n + \Delta\varepsilon_{n+1}$
2. Compute $D_s(E_e,\nu_e,c_{n+1},N_0)$ and $\Delta\sigma = D_s:\Delta\varepsilon_{n+1}$
3. Compute $p_{n+1}$ and $q_{n+1}$ and $F_d(p_{n+1},q_{n+1},c_{n+1})$
4. If Damage Surface, $F_d < 0$. YES: EXIT

   ELSE: *Evolve micro-cracks*
5. Compute incremental micro-crack growth

$$c_{n+1} = c_n + \Delta t\alpha(\sigma)\big|_n v_R\big|_{n+1}$$



ornl
Bringing Science to Life

# Material Point Constitutive Algorithm

6. Update the Moduli $D_s$ using, $c_{n+1}$

7. Update stresses using incremental constitutive equation

$$\sigma_{n+1} = \sigma_n + D_e\big|_{n+1} : \Delta\varepsilon_n + \frac{\partial D_e\big|_{n+1}}{\partial c_{n+1}}\left(c_{n+1} - c_n\right) : \varepsilon_{n+1}$$

8. EXIT

# Material Parameters

$E_0 = 4.4 \times 10^{11}$ Pa
$\nu_0 = 0.16$
$\rho = 3177$ Kg/m$^3$
$\sigma_0 = 0.0$
$\Gamma_R = 10.13$ N/m
$\mu = 0.26$

$N_0 = 10^{11}$ m$^{-3}$
$c_0 = 14$ μm

$\rho_0 = Nc_0^3 = 2.744 \times 10^{-4}$

Representative of SiC material

# Uniaxial Strain Test

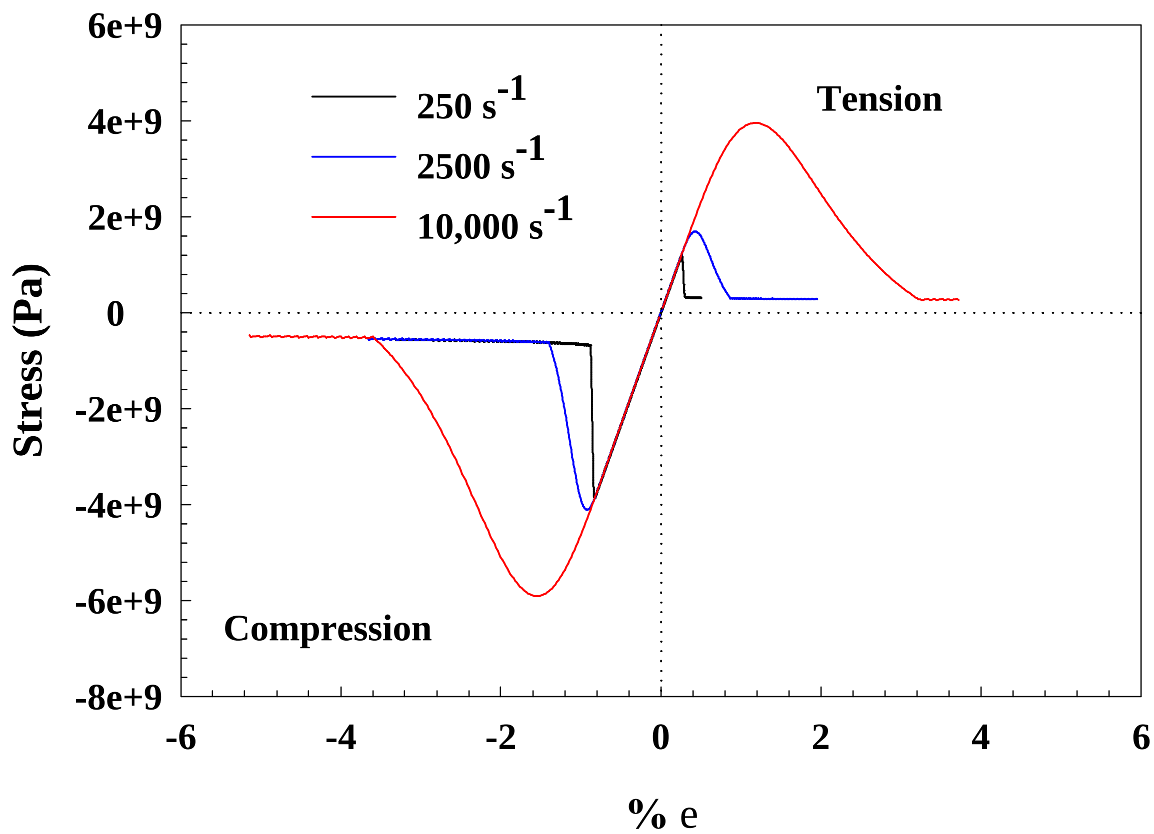


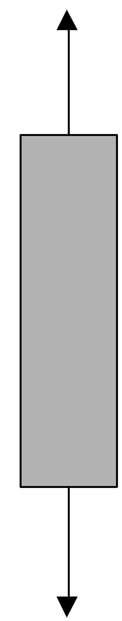



ornl
Bringing Science to Life

# Uniaxial Strain Tension

Load path in the (p,q,c) space

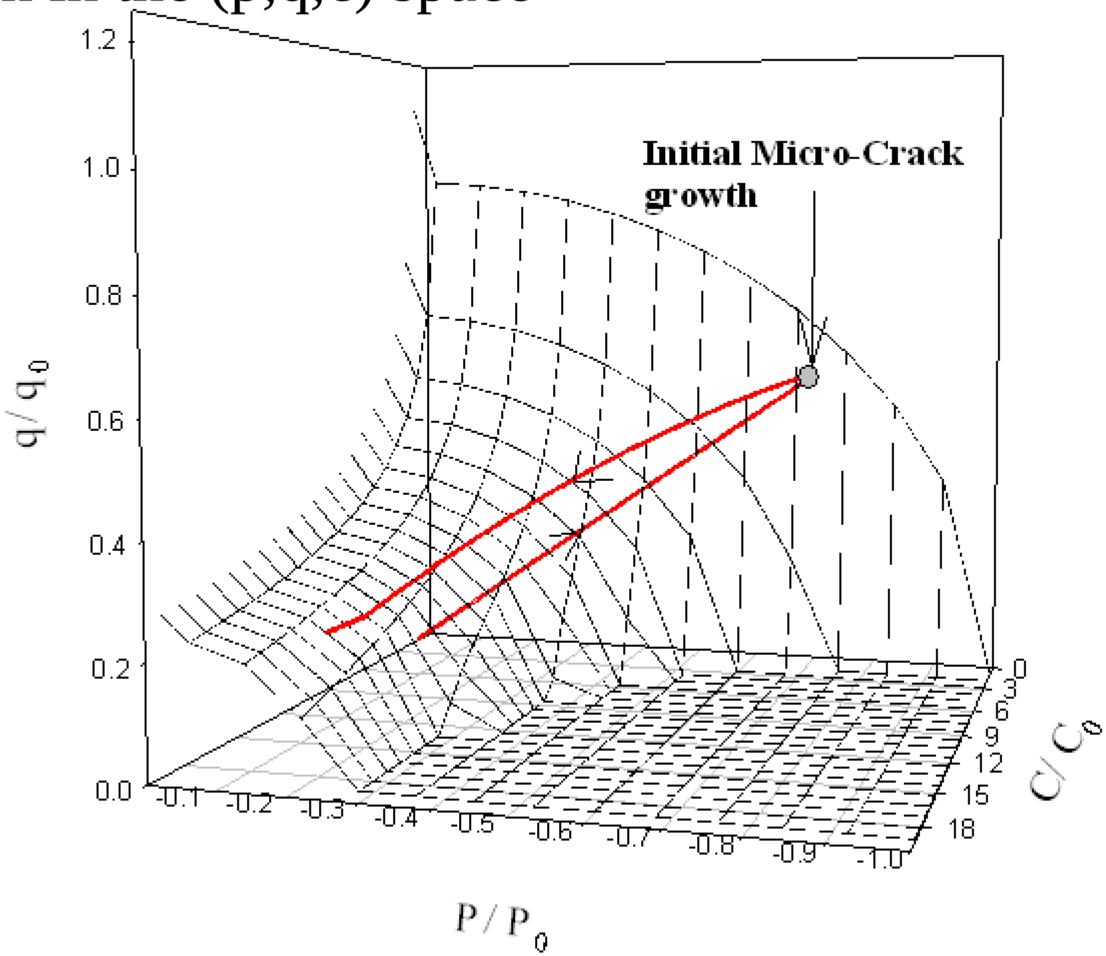




Bringing Science to Life

# Uniaxial Strain Compression

Load path in the (p,q,c) space

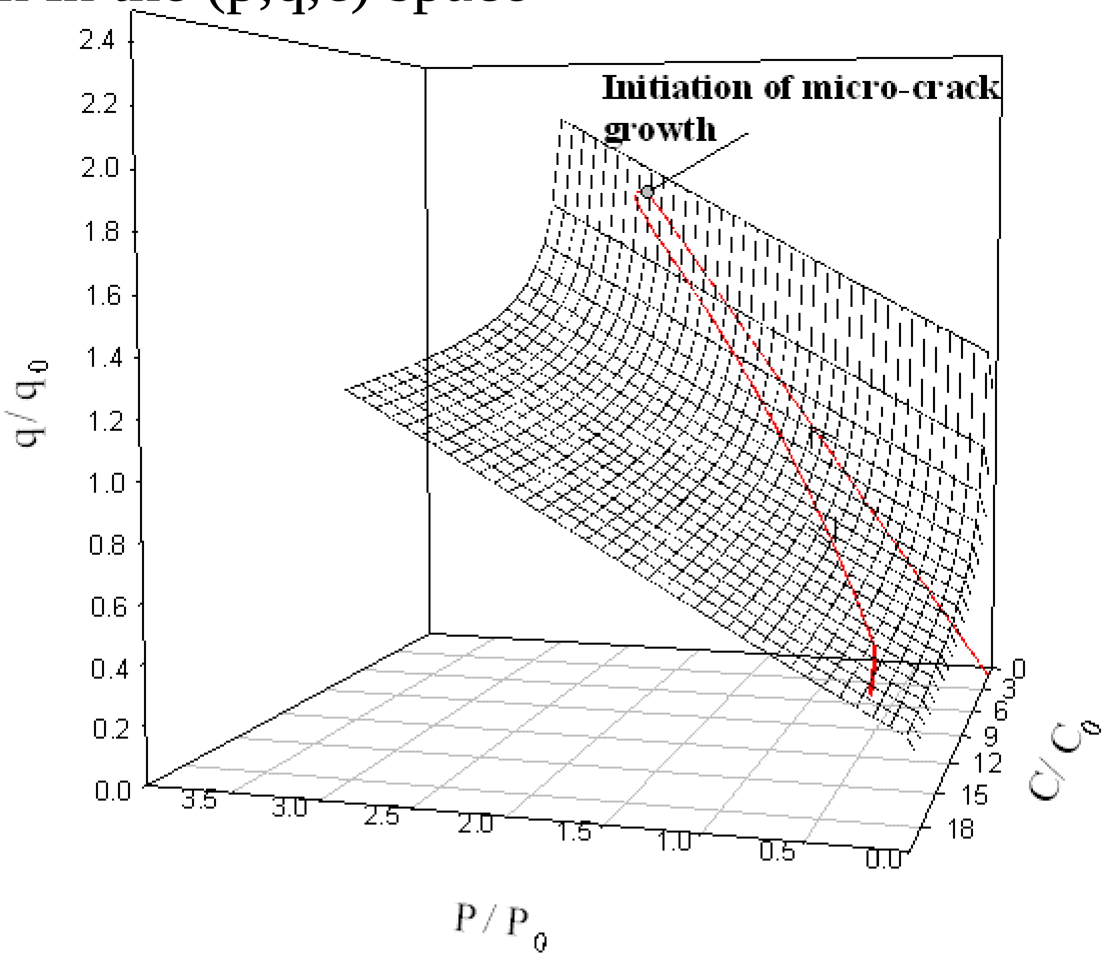




Bringing Science to Life

# Softening – Uniaxial Strain Tension

Effect of superimposed hydrostatic pressure on subsequent stress softening

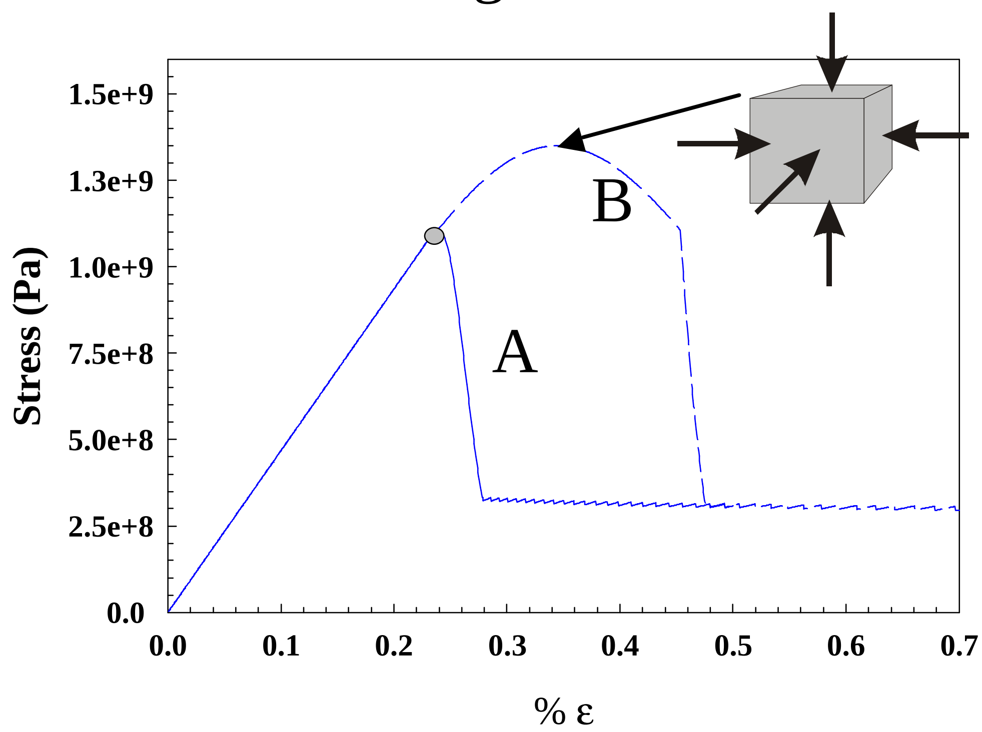


A – Stress path without superposed hydrostatic pressure

B – Stress path with superposed hydrostatic pressure after peak in curve A

# Softening –Triaxial Strain Tension

Effect of superimposed hydrostatic pressure on subsequent stress softening

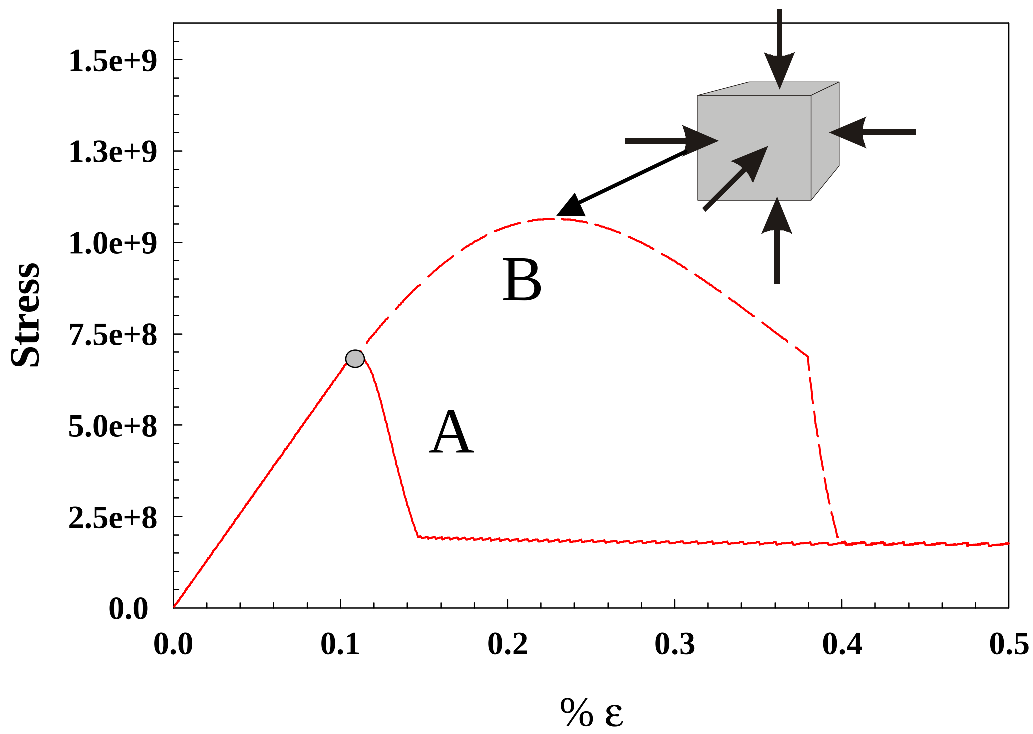


A – Stress path without superposed hydrostatic pressure

B – Stress path with superposed hydrostatic pressure after peak in curve A

# Experimental Measurement of $G_R$

- The various energy dissipating damage mechanisms are expected to result in an R-curve like crack growth in RFCC's (Gaggar & Broutman, 1975)

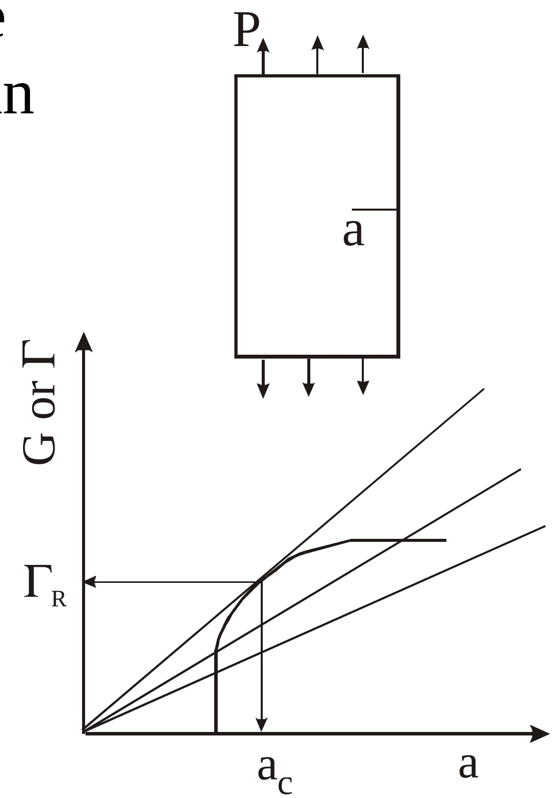


- Device a SEN or a DCB test specimen program to evaluate the R-Curve for the composite



ornl
Bringing Science to Life

# Calibration of N and $c_0$

- Use the experimentally obtained P-u curve to calibrate the model
- Numerically simulate the test to reproduce the P-u curve and obtain representative values for N and $c_0$

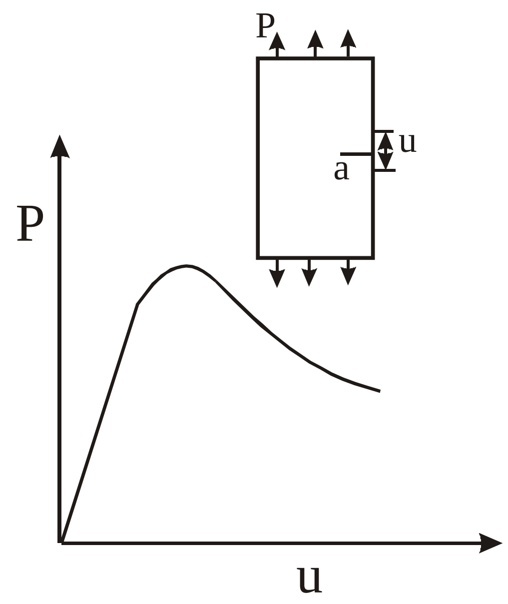

# Delamination Modeling Using Cohesive Elements

**Pakal Rahul-Kumar**
**Sunil Saigal***
**Anand Jagota†**

*** Carnegie Mellon University**
**† CR&D, The DuPont Co.**

# Delamination Failure of Composites

- Failure in RFC composites is observed to occur through delamination between plies in the composite
- Delamination involves propagation of crack surfaces accompanied by energy dissipation

# Delamination - Cohesive Elements

- Energy dissipation during delamination occurs within the cohesive zone located ahead of propagating crack front

- In computational modeling of delamination, cohesive elements are a powerful tool to model automatic failure initiation and subsequent propagation

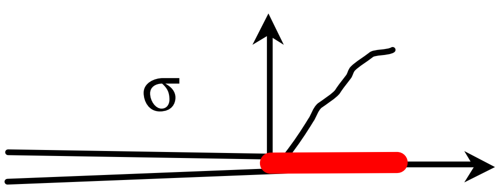


Cohesive Zone

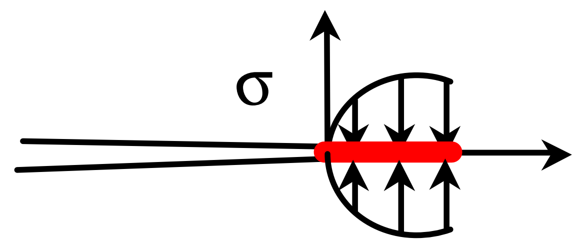


Cohesive Element

# Cohesive Zone Potentials

- Cohesive Zone Potentials, $\phi$, are used to represent energy dissipation occurring during delamination

$$\phi_{XN}(\Delta_n, \Delta_{t1}, \Delta_{t2}) = \Gamma_0\left[1-\left(1+\frac{\Delta_n}{\delta_{cr}}\right)\exp\left(-\frac{\Delta_n}{\delta_{cr}}\right)\exp\left(-\frac{\Delta_{t1}^2+\Delta_{t2}^2}{\delta_{cr}^2}\right)\right]$$

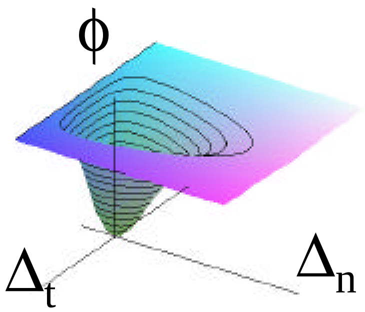


- Potentials allow for coupling of deformation between the normal and tangential modes of delamination

# Cohesive Zone Tractions

- Tractions across crack faces are obtained as

$$T_n = -\frac{\partial\phi(\Delta_n, \Delta_{t1}, \Delta_{t2})}{\partial\Delta_n}, \text{etc}$$

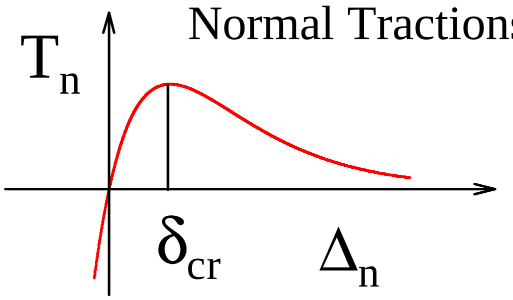


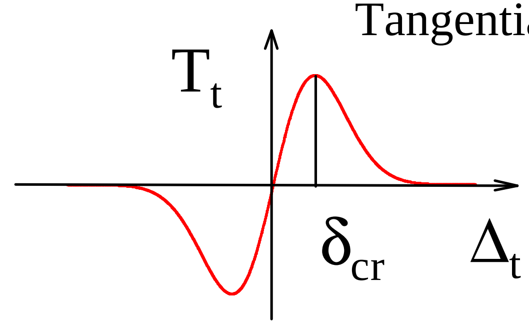


- Model parameters are $\Gamma_0 = \int_0^{\delta_{cr}} T_n(\Delta_n, \Delta_{t1}, \Delta_{t2})\, d\Delta_n$

$\delta_{cr}$ - Critical opening displacement

# Dynamic Crack growth in a DCB

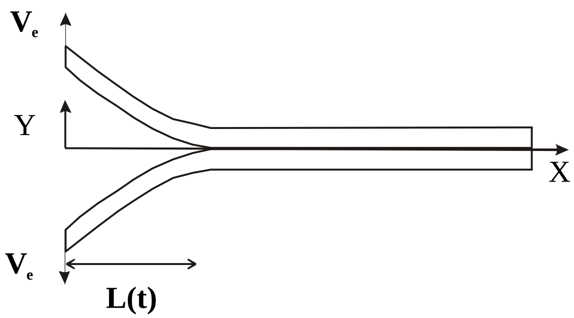


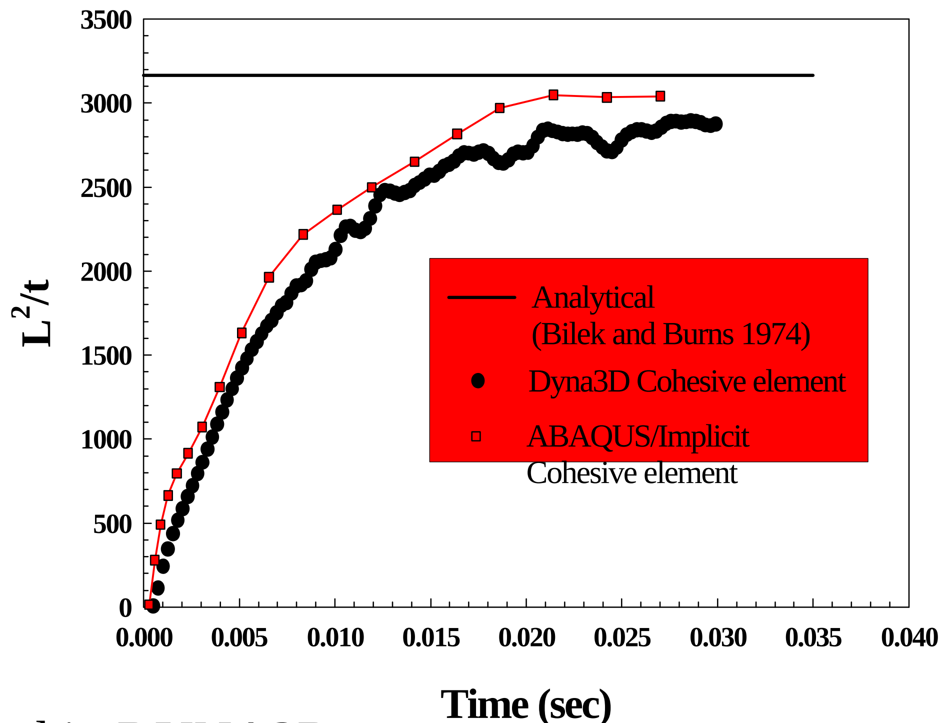


- Cohesive element implemented in DYNA3D
- Verifies our implementation of cohesive element

# Future Efforts

- Develop better approximations to micro-crack growth velocity based on analytical solutions for a penny-shaped crack under dynamic loading conditions

- Consider effects of fibers and surrounding micro-cracks on energy release rate and corresponding damage surfaces
  - Stang 1986 and Pijauder-Cabot & Bazant 1991
  - Effects of secondary tensile cracks in compression

- Obtain a plane stress formulation for use with shell elements
  - $\sigma_{33} = 0$, $\Delta\varepsilon_3$ in not kinematically specified

# Future Efforts

- Investigate into the reduced integrated versus the fully integrated shell formulations to be used with the model effectively
  - Belytschko-Tsay element
  - Hughes-Liu element

- Formalize the experimental program for the calibration of the model

- Simulate the quasi-static and dynamic RFC composite crush tube tests

# Modeling of P4 Preform

John D. Allen and Srdan Simunovic

Computational Materials Science Group
Oak Ridge National Laboratory

# P4 Microstructure Model

- Model currently simulates fiber deposition, only
- Complete process model should include preform compression, resin infusion and curing
- Model is used for linking of manufacturing process to resulting mechanical properties
- P4 fiber deposition simulation provides information for micro-mechanical model to account for characteristic distributions of preform and fiber properties

# Fiber Deposition Process

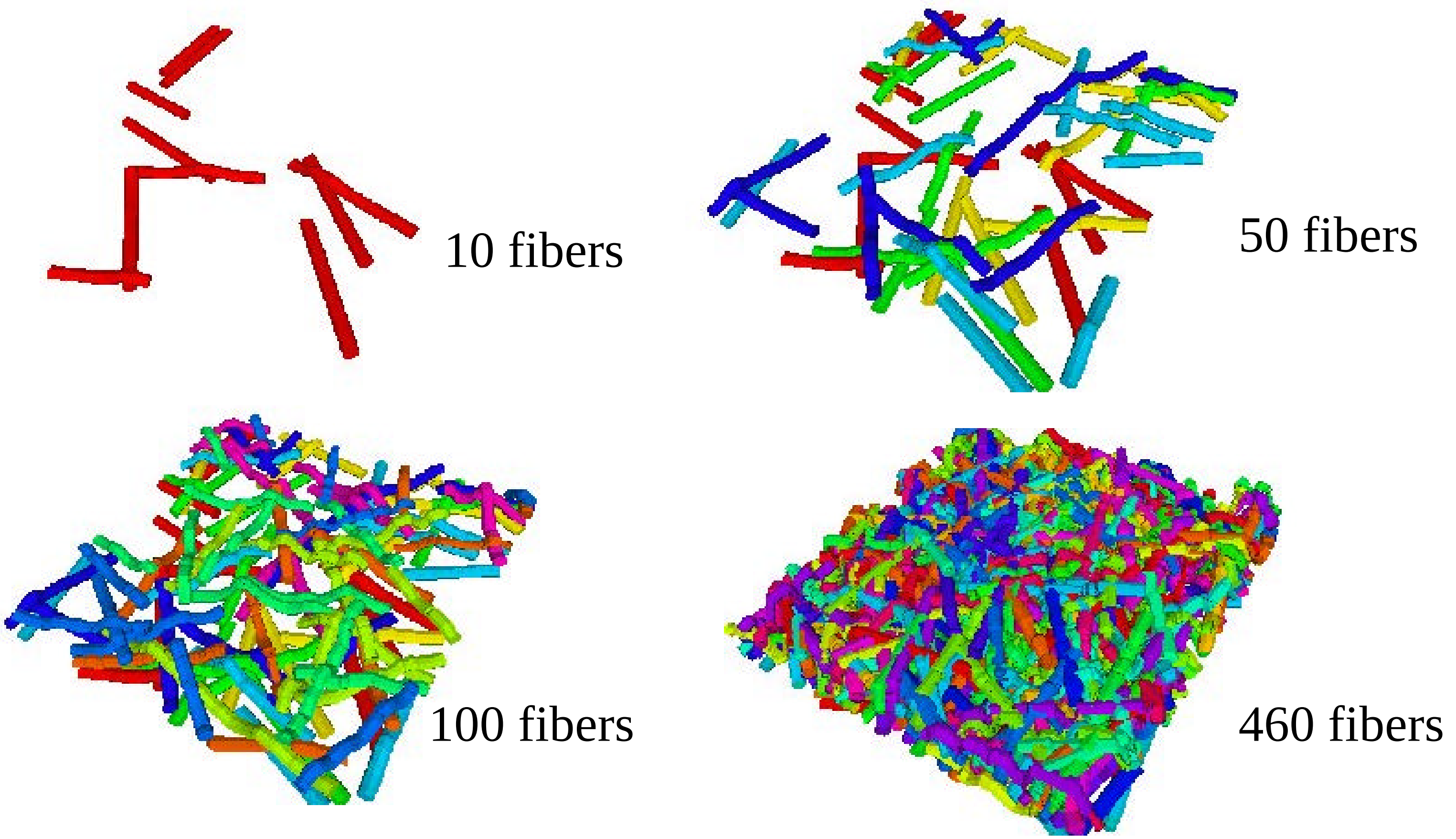

# Fiber Deposition Model

- Process variables used in simulation:
  - Spatial and orientation distributions
  - Fiber length, cross-section area, filamentization, flexibility, cross-section deformation
- Programmed deposition results in characteristic fiber property distributions
- Process variables ultimately determine distribution of effective material properties

# P4SIM Program Control

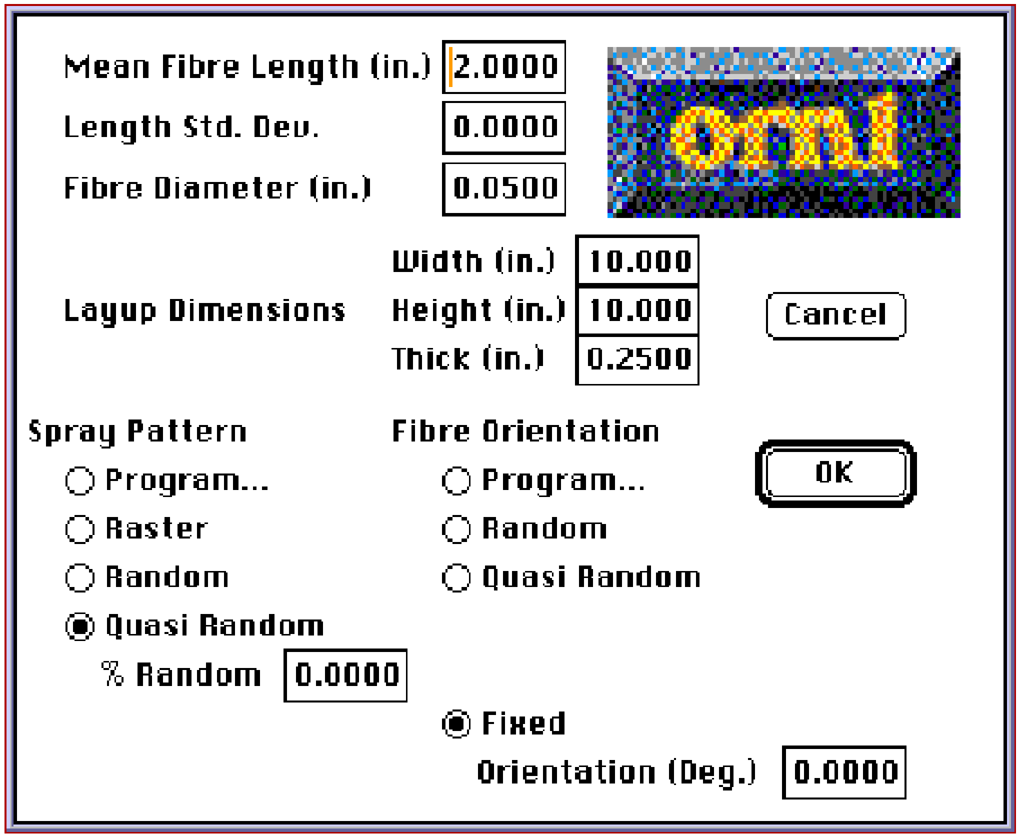




Bringing Science to Life

# Preform Analysis

- Fiber-fiber and fiber-resin contact areas indicate interaction between constituents

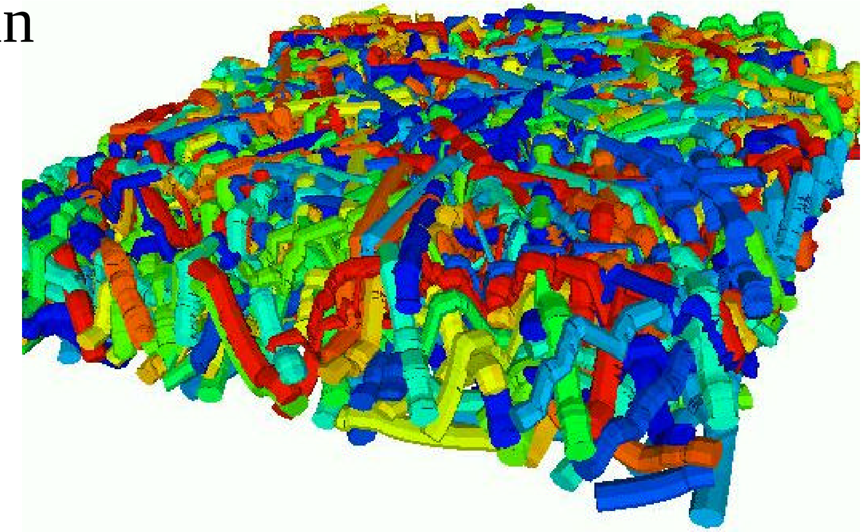

- Preform sectioning in longitudinal and through-thickness direction indicate effective lamina properties distributions, and representative volumes, and delamination paths

# Preform Analysis

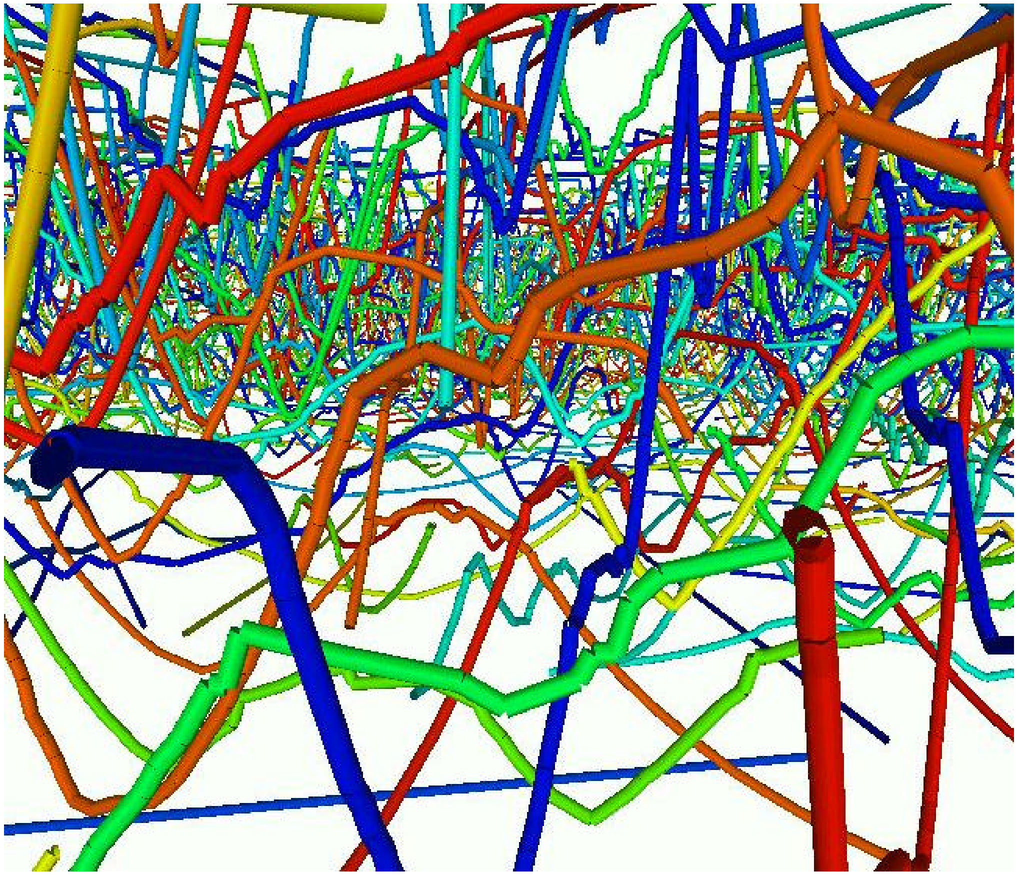

- Line representation is used for analysis of longitudinal fiber properties
- Free volume analysis is used for determination of characteristic resin volume distribution

# Preform Measures

- Implemented measures:
  - Fiber-to-fiber contact area distribution
  - Fiber-to-resin contact area distribution
  - Fiber longitudinal shape distribution
  - Fiber cross-section distribution
- For random fiber deposition, fiber features vary in composite through-thickness direction

# Fiber-to-Fiber Contact Area

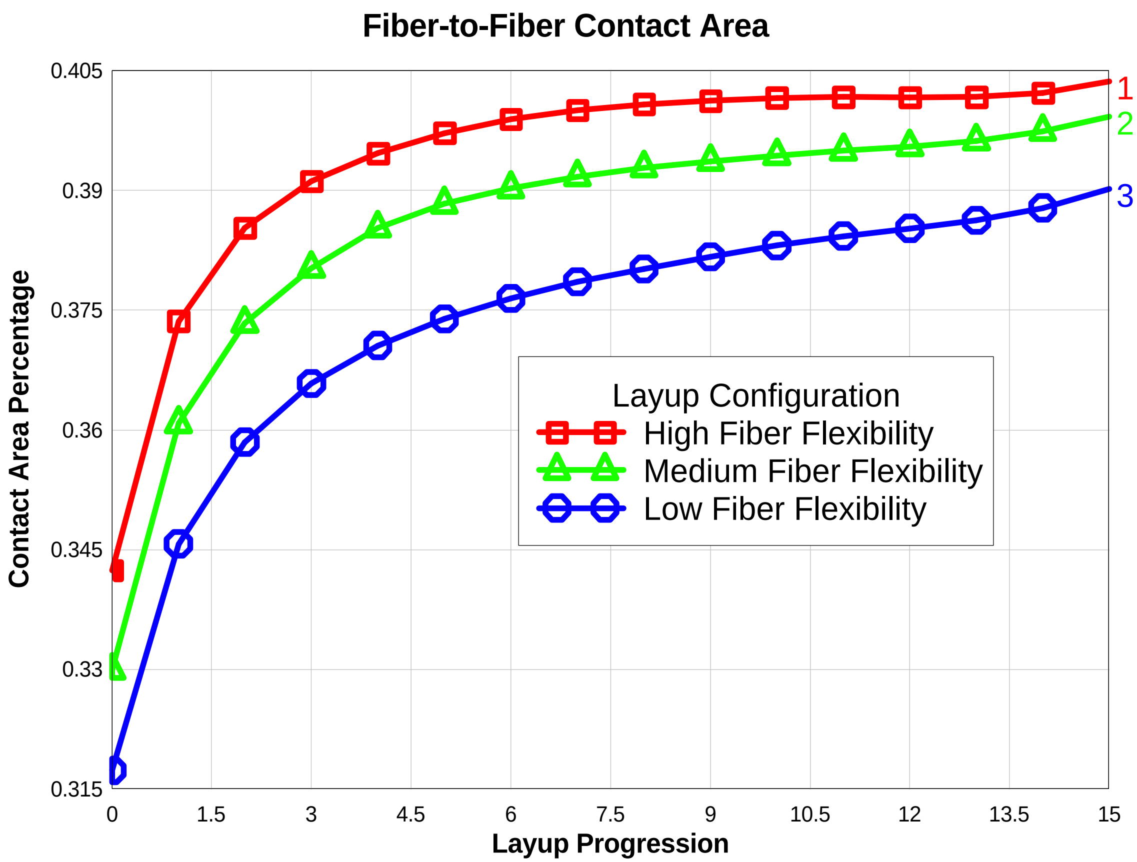


- Fiber flexibility in axial and cross-section directions control extent of contact



Bringing Science to Life

# Fiber Shape Analysis - Wavelet Spectrum

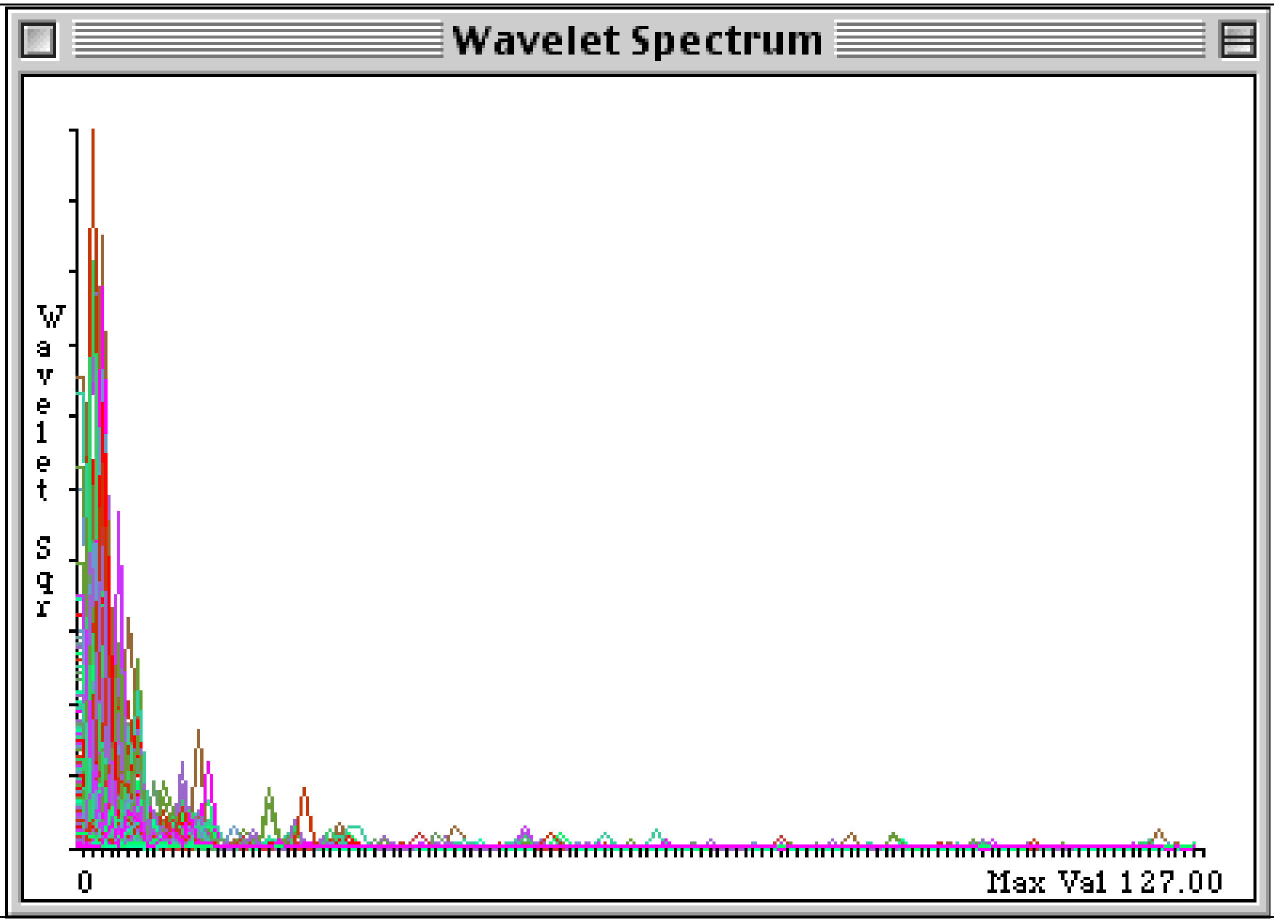

# Fiber Shape Analysis - Power Spectrum

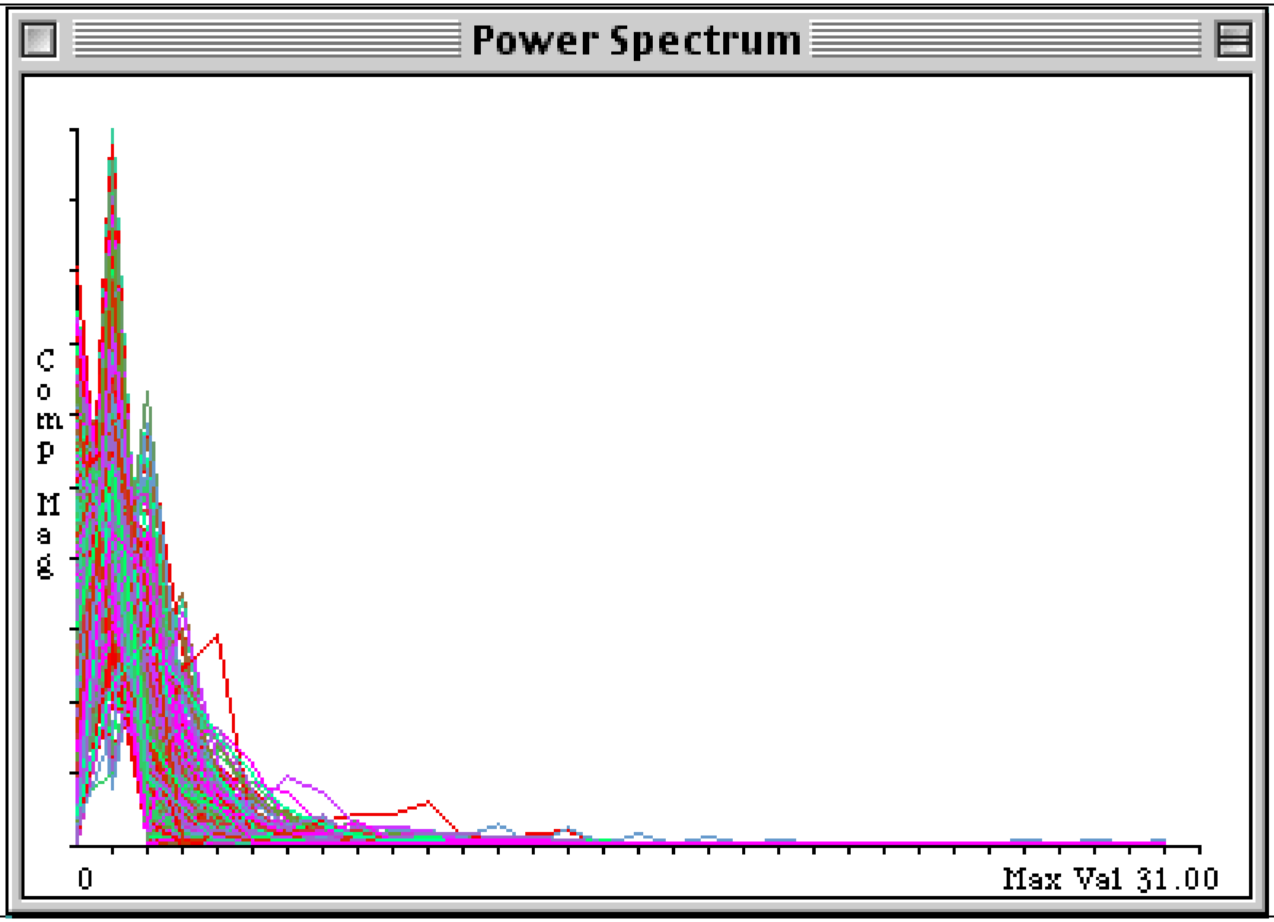

# Fiber Shape Analysis

- Plots are continuously updated during layup
- Fibres lying lowest in the layup bear the lowest frequency components (and fewer components in general)
- Fibers lying higher in the layup bear the highest frequencies since they must adjust to ever more complicated "substrates”
- Frequencies stabilize after certain thickness is reached

# Relevance to Material Modeling

- Fiber shape characterization is used for determination of equivalent fiber shape distributions in micro-mechanics-based model
- Fiber shape distribution and fiber-to-fiber/resin contact is used for solution of single fiber problem
- Material properties significantly vary in through-thickness direction and influence delamination
- Distribution of preform elastic properties can indicate representative volume of material